

Electronic supplementary Information (ESI) for Chemical Science.

This journal is © The Royal Society of Chemistry 2024

Regioselectivity Switches between Anthraquinone Precursor Fissions Involved in Bioactive Xanthone Biosynthesis

Xiao Jing Lv^{a,#}, Chun Zhi Ai^{b,#}, Li Rong Zhang^a, Xiu Xiu Ma^c, Juan Juan Zhang^d, Jia Peng Zhu^c, and Ren Xiang Tan^{a,d,*}

^a*State Key Laboratory Cultivation Base for TCM Quality and Efficacy, School of Pharmacy, Nanjing University of Chinese Medicine, Nanjing 210023, China*

^b*State Key Laboratory for Chemistry and Molecular Engineering of Medicinal Resources, Key Laboratory for Chemistry and Molecular Engineering of Medicinal Resources (Ministry of Education of China), Collaborative Innovation Center for Guangxi Ethnic Medicine, School of Chemistry and Pharmaceutical Sciences, Guangxi Normal University, Guilin 541004, China*

^c*School of Medicine and Holistic Integrative Medicine, Nanjing University of Chinese Medicine, Nanjing 210023, China*

^d*State Key Laboratory of Pharmaceutical Biotechnology, Institute of Functional Biomolecules, School of Life Sciences, Nanjing University, Nanjing 210023, China*

[#]Contributed equally to this work.

*Corresponding author: Ren Xiang Tan (rxtan@nju.edu.cn).

Table of contents

Experimental Procedures

General

Strains and culture conditions

Molecular biology experiments

Whole genome sequencing and bioinformatics analysis

Gene deletion

Heterologous expression

Substrate supplementation assay

Protein expression and purification

In vitro enzymatic assay

¹⁸O₂ labeling experiment

ICP-MS elemental analysis

Metal ion dependence assay

Phylogenetic analysis

Site-directed mutagenesis

Protein crystallization

Data collection and refinement

Isolation of monodictyphenone (**4a**) and emodinic acid
Generation of cephalanone F (**4b**) from chrysophanol (**2**)
Production of 11-hydroxy monodictyphenone (**5a**) from aloe emodin (**5**)
Chemical capture of chrysophanol hydroquinone (**3**) tautomers
Theoretical simulation

Supplementary Tables

Table S1. Annotation of the *bru* cluster in the *A. brunneoviolaceus* genome.
Table S2. Functional comparison of proteins encoded by the *bru*, *nsr*, *agn*, *sec*, and *dmx* gene clusters.
Table S3. Primers used in this study.
Table S4. Plasmids constructed for this study.
Table S5. ¹H (500 MHz) and ¹³C NMR (125 MHz) data of monodictyphenone (**4a**).
Table S6. ¹H NMR (500 MHz) data of cephalanone F (**4b**).
Table S7. ¹H NMR (500 MHz) data of 11-hydroxy monodictyphenone (**5a**) in CD₃OD.
Table S8. ¹H (600 MHz) and ¹³C NMR (150 MHz) data of **12** in CDCl₃.
Table S9. ¹H NMR (500 MHz) data of emodinic acid.
Table S10. X-ray data collection and refinement statistics.
Table S11. Interactivity comparison of substrate tautomers with BruN, BruN^{N441M}, and BTG13.

Supplementary Figures

Figure S1. The 88 biosynthetic gene clusters predicted by AntiSMASH (fungal version) in *A. brunneoviolaceus*.
Figure S2. Comparison of the *bru* cluster with its homologues in fungi.
Figure S3. Deletion of the *bruN* gene from the *A. brunneoviolaceus* genome.
Figure S4. SDS-PAGE analysis of BruM (38.6 kDa), BruN (53.0 kDa), and BTG13 (WAU16873.1, 51.6 kDa).
Figure S5. LC-MS assay for the chrysophanol (**2**)-derived products from the *in vitro* enzymatic reactions.
Figure S6. LC-MS analyses (negative ion mode) of ring-opened products of emodin (**1**), aloe emodin (**5**), physcion (**6**), and rhein (**7**), after individually exposed to BruMN in presence of NADPH.
Figure S7. Conversion rate comparison of BruMN catalyzed fission of **1**, **2**, and **5–7**.
Figure S8. Multiple sequence alignment of BruN with its homologs using ClustalX2.1.
Figure S9. Structural comparison of BruN, BruN^{N441M}, BTG13, and BruN^{N441F/Q437A/V347L}.
Figure S10. SDS-PAGE analysis of BruN and some of its variants.
Figure S11. HPLC profiling of chrysophanol (**2**)-derived products under the catalysis of some of single-site BruN variants in the presence of BruM and NADPH.
Figure S12. SDS-PAGE analysis of BTG13 and its variants.
Figure S13. HPLC profiling for monodictyphenone (**4a**) and cephalanone F (**4b**) forming possibly from chrysophanol (**2**) under the catalysis of BTG13 variants in the presence of BruM and NADPH (as cofactor).

Figure S14. HPLC profiling of chrysophanol (**2**)-derived products under the catalysis of saturation mutants on site N441 in BruN in the presence of BruM and NADPH.

Figure S15. HPLC profiling of chrysophanol (**2**)-derived products under the catalysis of some of double-site BruN variants in the presence of BruM and NADPH.

Figure S16. HPLC profiling of chrysophanol (**2**)-derived products under the catalysis of N441-to-phenylalanine muted BruN variants in the presence of BruM and NADPH.

Figure S17. HPLC profiling of chrysophanol (**2**)-derived products under the catalysis of some of multiple-site BruN variants in the presence of BruM and NADPH.

Figure 18. HPLC profiling for monodictyphenone (**4a**) and cephalanone F (**4b**) generating from chrysophanol (**2**) under the catalysis of BruN variants.

Figure S19. Identification of the BruN-bound iron ion.

Figure S20. SDS-PAGE analysis of purified BruN variants (53.0 kDa) resulting from mutating the conserved and functionally significant sites as co-indicated by the multiple sequence alignment (see Figure S8) and the docking result of BruN with chrysophanol hydroquinone (**3**).

Figure S21. Activity comparison for BruN and its mutants in catalyzing the chrysophanol (**2**) cleavage in the presence of BruM and NADPH.

Figure S22. Compound **12** was synthesized from chrysophanol (**2**) to confirm the keto-enol tautomerism that might be involved in the enzymatic fission process.

Figure S23. Conformations of **3a** and **3b** with their relative energies obtained at B3LYP level.

Figure S24. HR-ESI-MS spectra of monodictyphenone (**4a**) produced in atmospheric $^{16}\text{O}_2$ (A) and $^{18}\text{O}_2$ (B).

Figure S25. ^1H NMR spectrum of monodictyphenone (**4a**).

Figure S26. ^{13}C NMR spectrum of monodictyphenone (**4a**).

Figure S27. HR-ESI-MS spectrum of cephalanone F (**4b**).

Figure S28. ^1H NMR spectrum of cephalanone F (**4b**).

Figure S29. HR-ESI-MS spectrum of 11-hydroxy monodictyphenone (**5a**).

Figure S30. ^1H NMR spectrum of 11-hydroxy monodictyphenone (**5a**) in CD_3OH .

Figure S31. HR-ESI-MS spectrum of **12**.

Figure S32. ^1H NMR spectrum of **12** in CDCl_3 .

Figure S33. ^{13}C NMR spectrum of **12** in CDCl_3 .

Figure S34. HR-ESI-MS spectrum of emodinic acid.

Figure S35. ^1H NMR spectrum of emodinic acid.

References

Experimental Procedures

1. General

The synthesis of oligonucleotide primers (Table S3) and DNA sequencing were accomplished by TsingKe Biotech Co., Ltd. (Nanjing, China). HR-ESI-MS data were measured on an Agilent 6546 Accurate-Mass Q-TOF LC-MS spectrometer, with a ZORBAX RRHD SB-C18 column (2.1×100 mm, 1.8 μm, Agilent Technologies). NMR spectra were recorded on a Bruker AV-500 or AV-600 spectrometers in acetone-*d*₆ (unless stated otherwise). HPLC (high performance liquid chromatography) analysis was carried out on an Agilent Technologies 1260 Infinity LC System, equipped with a DAD detector by a Proshell 120 EC-C18 (150 × 4.6 mm, 4 μm). Semi-preparative HPLC was performed on an Agilent 1260 by an Eclipse XDB-C18 column (250 × 9.4 mm, 5 μm).

2. Strains and culture conditions

The fungus *Aspergillus brunneoviolaceus* FB-2 (*A. brunneoviolaceus*) was isolated from the fresh stool of a healthy individual, and maintained on potato dextrose medium containing 2% agar (PDA) at 28 °C and stored at –80°C with 20% glycerol.¹ For the isolation of the fungal polyketides such as brunneoxanthone E, the fresh mycelium was inoculated into malt extract (ME) medium (20 g/L malt extract, 20 g/L sucrose and 1 g/L peptone) and cultivated for 7 days at 28°C with agitation (130 rpm, DZ-900 agitator, Taicang Qiang Le Experimental Equipment Co., Ltd.).¹ *Aspergillus oryzae* NSAR1 (*niaD*[–], *sC*[–], Δ *argB*, and *adeA*[–]) was used as the host for heterologous expressions. *A. oryzae* and its transformants were cultured at 28°C for 5 days in DPY agar plate (20 g/L dextrin, 10 g/L polypeptone, 5 g/L yeast extract, 5 g/L KH₂PO₄, 0.5 g/L MgSO₄·7H₂O, and 2% agar), then transferred to CDM medium (2 g/L soluble starch, 30 g/L saccharose, 1 g/L polypeptone, 20 g/L maltose, 1 g/L yeast extract, 3 g/L NaNO₃, 1 g/L K₂HPO₄, 0.5 g/L MgSO₄·7H₂O, 0.01 g/L FeSO₄·7H₂O, 0.55 g/L CaCl₂) followed by agitation at 130 rpm for 6 days. Substrate chrysophanol (**2**) was added into the culture on day 2 of cultivation, and cultured for 4 days at 28°C for the product isolation. *Escherichia coli* DH5α was used as a host for molecular cloning. At 37°C, *E. coli* cells carrying each plasmid were agitated at 180 rpm in Luria-Bertani (LB) medium containing 100 μg/mL ampicillin or 50 μg/mL kanamycin depending on the selection purpose.

3. Molecular biology experiments

After cultured on PDA for 2 days, the mycelia of *A. brunneoviolaceus* and its Δ *bruN* mutant (approximately 0.2 g each) were collected, flash-frozen in liquid nitrogen and triturated using a tissue grinder; and genomic DNA was extracted according to the manufacturer's instructions of Rapid Fungi Genomic DNA Isolation Kit (Sangon Biotech). For the total RNA extraction, *A. brunneoviolaceus* was cultivated in ME medium at 28°C for 3 days, the mycelia were obtained by centrifugation and dried out with filter paper, after flash-frozen in liquid nitrogen and crushed using a tissue grinder, the dried powder was dissolved in 1 mL Trizol Reagent (Vazyme Biotech), and the fungal RNA was extracted according to the manufacturer's instructions, with the residual genomic DNA digested with RNase-free DNase I (Thermo Fisher Scientific)

at 37°C for 4 h. The cDNA synthesis was performed by Reverse transcription PCR (RT-PCR) using RevertAid First Strand cDNA Synthesis Kit (Thermo Fisher Scientific) with Oligo-dT primers, following the instruction from the user manual. The concentration of genomic DNA and total RNA were determined by Thermo Fisher Scientific U-3000 NanaDrop 2000C. Phanta Max Super-Fidelity DNA Polymerase, ClonExpress Ultra (or Multis) One Step Cloning Kit and 2×Rapid Taq Master Mix (Vazyme Biotech Co., Ltd) were applied for the amplification of target genes, constructions of expression vectors, and verification of transformants. The DNA restriction enzymes were used as recommended by the manufacturer (New England Biolabs, NEB). The plasmid pET28a (+) was used as the vector for recombinant protein expression in *E. coli* transetta (DE3) (TransGen Biotech, Beijing). The plasmids were extracted by SanPrep Column Plasmid Mini-Preps Kit (Sangon Biotech Co., Ltd).

4. Whole genome sequencing and bioinformatics analysis

The whole genome sequencing of *A. brunneoviolaceus* was carried out by Benagen Tech Solutions Company Limited (Wuhan, China) with both Illumina NovaSeq and Oxford Nanopore PromethION sequencing platform. The NECAT (<https://github.com/xiaochuanle/NECAT>) sequence assembly system was used to produce 9 contigs, covering about 36.6 Mb. The function of coding sequence was predicted by AUGUSTUS (<http://bioinf.uni-greifswald.de/webaugustus/>). In the genome, the polyketide biosynthetic gene clusters were analyzed by antiSMASH fungal version (<https://fungismash.secondarymetabolites.org/>),² with the protein functions further predicted by 2ndFind (<http://biosyn.nih.go.jp/2ndfind/>). The multiple sequence alignments were performed by DNAMAN.

5. Gene deletion

To knock out the target gene, homologous recombination based on split-marker strategy was used.³ Briefly, the entire gene-deletion cassette involved hygromycin-resistance marker (hygromycin phosphotransferase gene, *hph*), the 5' (upstream) and 3' (downstream) flanking sequences of target gene (Figure S3). It was divided into two fragments, *U-hph1* (5' flanking sequence of target gene and forward part of *hph*) and *hph2-D* (backward part of *hph* and 3' flanking sequences of target gene). About 1.8 kb of 5' and 3' flanking sequences of target gene were PCR-amplified from the fungal genomic DNA. Split *hph* fragments (*hph1* and *hph2*) were PCR-amplified from plasmid pSH75, which contained the *PtrpC* promoter, *hph* gene, and *TtrpC* terminator. The fragments, 5' flanking sequence and *hph1*, were inserted into the KpnI-linearized vector pTAex3 to generate recombinant plasmid pTAex3-*U-hph1* through homologous recombination with ClonExpress MultiS One Step Cloning Kit (Vazyme Biotech). The pTAex3-*hph2-D* was generated in the same way. The fragments *U-hph1* and *hph2-D* were PCR-amplified in larger quantities from pTAex3-*U-hph1* and pTAex3-*hph2-D*, respectively.

A. brunneoviolaceus was cultured on PDA for 24 h to produce the fresh mycelia, which were inoculated to YPED (20 g/L sucrose, 10 g/L yeast extract, 10 g/L polypeptone and 10 g/L casein hydrolyzate) followed by agitation at 130 rpm for 30 h at 28 °C. The harvested thallus was co-treated with 20 mg/mL lysing enzyme (Sigma-

Aldrich, L1412) and 20 mg/mL lysoenzyme from chicken egg (SigmaAldrich, L6876) followed by incubation at 28 °C for 2 h to produce protoplasts. The protoplasts were collected via centrifugation at 4,200 rpm for 20 min, washed successively with MN buffer (0.3 M MgSO₄·7H₂O and 0.3 M NaCl) and KTC buffer (1.2 M KCl, 50 mM CaCl₂ and 10 mM Tris-HCl, pH 7.5). The treated protoplasts were transformed with the two split-marker gene deletion cassettes *U-hph1* and *hph2-D* by the polyethylene glycol (PEG)-mediated transformation strategy. After the transformation, the protoplasts were poured onto the PDA plate which supplemented with 200 µg/mL of hygromycin B for the resistance screening. Diagnostic PCR using primers diagnostic F/R (Diag F/R) listed in Table S3 was carried out to identify the mutants.

6. Heterologous expression

For heterologous expression in *A. oryzae*, plasmids pTAex3 and pBARI were used as backbones to carry target genes. Each gene was amplified from the genomic DNA (gDNA) of *A. brunneoviolaceus* using primers in Table S3. Based on homologous recombination, the DNA fragments *bruM* and *bruN* were initially ligated into the KpnI-digested pTAex3 vector using ClonExpress Ultra One Step Cloning Kit (Vazyme Biotech) according to the manufacturer's protocol. For the construction of *bruM* into pBARI, the resultant fragment including the *amyB* promoter (*PamyB*) and *amyB* terminator (*TamyB*) was amplified from the pTAex3-*bruM* plasmid and ligated into SmaI-digested pBARI vector to produce pBARI-*bruM* (Table S4).

The first plasmid was transformed into *A. oryzae* NSAR1 and the resultant transformant was further transformed using the second plasmid by the PEG-mediated method. According to the result of PCR, the positive transformants were verified, and then fermented in CDM.

7. Substrate supplementation assay

Each transformant was at 28°C cultivated in 400 mL of CDM medium while shaken at 130 rpm for 2 days. To the culture, 5 mg of chrysophanol (**2**, always dissolved in DMSO) was added followed by a 4-day incubation. The broth was extracted with ethyl acetate twice and concentrated *in vacuo*. The dried extracts were dissolved in methanol for the LC-MS analysis using the duration-dependent methanol/water (containing 0.1% formic acid) gradients (0→10 min, 5:95→35:65; 10→35 min, 35:65→100:0; 35→40 min, pure methanol), at a flow rate of 0.2 mL/min with a DAD detection.

8. Protein expression and purification

The full-length *bruN* gene was PCR-amplified from the cDNA of *A. brunneoviolaceus* with primers pET28a-*bruN*-F/pET28a-*bruN*-R (Table S3). The *bruN* gene was ligated into the *Nde*I and *Hind*III linearized pET28a vector using ClonExpress Ultra One Step Cloning Kit. The resulting plasmid was sequenced to verify its identity, and the verified plasmid was transformed into *E. coli* BL21 (DE3) for His₆-tagged protein induction and purification. Specifically, the obtained transformant was grown at 37 °C for 12 h at 220 rpm in 5 mL of LB medium supplemented with 50 µg/mL kanamycin. The culture was inoculated into 400 mL of fresh LB medium containing 50

$\mu\text{g/mL}$ kanamycin and incubated at 37°C until the optical density at 600 nm (OD_{600} value) reached 0.6~0.8. Isopropylthio- β -D-galactoside (IPTG) was added to the culture at 0.2 mM to induce protein expression, and was incubated at 16°C for 18 h at 220 rpm. The cells were collected at 4°C via centrifugation at 8000 rpm for 10 min, re-suspended in 20 mL lysing buffer (200 mM NaCl, 5 mM imidazole, 25 mM Tris-HCl, pH 8.0), and disrupted through sonication on ice for 30 min. The lysate was centrifuged at 4°C at 12000 rpm for 30 min to remove the cellular debris. The supernatant was filtered through 0.45 μm filter (Merck millipore) and applied to Ni^{2+} -chelating affinity chromatography to purify protein, using the imidazole-increased (50–500 mM) buffer (200 mM NaCl, 25 mM Tris-HCl, pH 8.0). The fraction containing the desired protein was desalted and concentrated using 10 KD centrifugal cutoff filters (Merck Millipore) by centrifugal filtration. The purity of BruN protein was analyzed by SDS-PAGE and the concentration was determined by U-3000 NanaDrop 2000C (Thermo Fisher Scientific). The intron-free *bruM* gene was amplified using cDNA from *A. brunneoviolaceus*. The PCR-amplified DNA was ligated into linearized pET28a by homologous recombination method, and the obtained plasmid was confirmed through DNA sequencing. The *BTG13* gene (NCBI Accession Number: WAU16873.1) was synthesized by TsingKe Biotech Co., Ltd. (Nanjing, China) and the pET28a-*BTG13* plasmid was constructed. The BruM and BTG13 proteins were expressed in *E. coli* BL21 (DE3) and purified as was BruN. All purified proteins were flash frozen in liquid nitrogen and stored at -80°C prior to being used.

9. *In vitro* enzymatic assay

The BruM and BruN co-catalyzed reaction was carried out with a total volume of 100 μL mixture containing 50 mM Tris-HCl buffer (pH 7.5), 15 μM BruM, 15 μM BruN, 250 μM chrysophanol (**2**), and 2 mM NADPH. After incubated at 30°C for 2 h, the reaction mixture was quenched by adding an equal volume of acetonitrile. After the vortex mixing and centrifugation, the obtained supernatant was analyzed by LC-MS. Likewise evaluated were the BruM and BTG13 co-catalysis. Under the same condition but without BruM, the cofactors NADPH, NADH, FAD, and FMN were individually added into the reaction system to test whether or BruN catalyzed the ring opening of chrysophanol (**2**) independently. In the enzymatic (BruN) reaction, the cofactor was replaced by $\text{Na}_2\text{S}_2\text{O}_4$ to test whether BruN catalyzed the cleavage of chrysophanol hydroquinone (**3**) resulting from the $\text{Na}_2\text{S}_2\text{O}_4$ reduction of **2**. To probe the lability of **3**, the reactants were taken for an in-process analysis, 2 and 10 min after **2** was exposed simultaneously to BruM and NADPH. In the BruM and BruN co-catalytic reaction mixture, emodin (**1**), aloe emodin (**5**), physcion (**6**), rhein (**7**), and emodin 8-O- β -D-glucopyranoside (**8**) were added separately to evaluate the substrate specificity of the enzyme pair. The LC-MS analysis was performed using the duration-dependent methanol/water (containing 0.1% formic acid) gradients (0 \rightarrow 10 min, 5:95 \rightarrow 35:65; 10 \rightarrow 35 min, 35:65 \rightarrow 100:0; 35 \rightarrow 40 min, pure methanol). The reaction condition and analytical condition was performed as illustrated unless stated otherwise.

10. $^{18}\text{O}_2$ labeling experiment

Added to a penicillin bottle were 410 μL of 50 mM Tris-HCl buffer (pH 7.5), 10

μL of 10 mM chrysophanol (**2**) and 20 μL of 50 mM NADPH. A highly pure nitrogen stream was bubbled through the bottle to thoroughly remove the atmospheric O_2 , being sealed with the rubber stopper. With that, the 97% $^{18}\text{O}_2$ gas (Wuhan Yi Si Tuopu Technology Co., Ltd.) was introduced into the bottle via a syringe needle. Finally, 40 μL of BruM (9 mg/mL) and 20 μL of BruN (20 mg/mL) solutions were injected into the bottle via a syringe. After a 30-minute incubation at 30°C, an equal volume of acetonitrile was added to quench the reaction. The final reactant was mixed using a vortex mixer and centrifuged at 12000 rpm for 5 min at room temperature to afford a supernatant which was subjected to LC-MS analysis.

11. ICP-MS elemental analysis

As detailed elsewhere,⁴ BruN was subjected to nitrolysis with HNO_3 , and the obtained supernatant was analyzed by inductively coupled plasma mass spectrometry (ICP-MS) to quantify the metal concentration.

12. Metal ion dependence assay

Following the described procedure,⁵ a reaction mixture containing 50 mM Tris-HCl (pH 7.5), 15 μM BruM, 2 mM NADPH, 15 μM BruN, and 200 μM EDTA was incubated at 4°C for 30 min. To the incubated mixture, other metal ions were individually added at 5 mM followed by a 30-min incubation at 4°C. Aloe emodin, the most favorable substrate of BruN, was added at 250 μM to the mixtures with different metal ions added individually. After a 2-hour reaction at 30°C, the enzymatic reaction was analyzed as described in “*In vitro enzymatic assays*”.

13. Phylogenetic analysis

All the twelve BruN-like dioxygenases reported so far to catalyze the C_{10} – C_{10a} and/or C_{10} – C_{4a} cleavages of anthraquinones were included to make the phylogenetic analysis conclusive enough. Obtained from the NCBI database were the sequences of PhoJ (UPG58739.1) from *Diaporthe* sp.,⁶ AacuH (A0A1L9WLI9.1) from *Aspergillus aculeatus*,⁷ MdpL (C8VQ61.1) from *Aspergillus nidulans*,⁸ AgnL3 (A0A411PQN8.1) from *Paecilomyces variotii*,⁹ CPUR_05427 (M1WG92.1) from *Claviceps purpurea*,¹⁰ DmxR6 (A0A4P8DJZ3.1) from *Cryptosporiopsis* sp.,¹¹ BTG13 (PDB code: 7Y3W, WAU16873.1) from *Cercospora* sp.,⁴ GedK (Q0CCX5.1) from *Aspergillus terreus*,¹² TpcI (Q4WQY9.1) from *Aspergillus fumigatus*,¹³ PtaJ (A0A067XMK8.1) from *Pestalotiopsis fici*,¹⁴ and NsrF (A0A2I1C3U2.1) from *Aspergillus novofumigatus*.¹⁵ Subsequent sequence alignment was performed using Clustal X2.1 online version, and the evolutionary tree was constructed through the neighbor-joining method using MEGA 5.0 software.¹⁶

14. Site-directed mutagenesis

Single-site BruN mutants were constructed by PCR amplification of mutated fragments using primers listed in Table S3 and pET28a-*bruN* plasmid as template. Double-site BruN mutants were obtained likewise using either the pET28a-*bruN* plasmid (if mutated sites are close enough), or pET28a-*bruN*-N441M, pET28a-*bruN*-N441W or pET28a-*bruN*-N441F plasmids if the sites are distant. In a similar manner, multiple-site BruN mutants were generated by selecting plasmids depending on the

distance of the mutated sites. The single-site BTG13 mutants (Figure S14) were constructed using pET28a-*BTG13* plasmid as template. The PCR products, mutated fragments, were purified and recombined using ClonExpress II One Step Cloning Kit (Vazyme Co., Ltd). Each mutation was verified by sequencing. The recombined plasmids were expressed in *E. coli* BL21 (DE3) and purified as described for BruN.

The catalytic competence of BruN mutants and BTG13 variants was individually evaluated by enzymatic reaction assays in the presence of BruM and NADPH, as were BruN and BTG13.

15. Protein crystallization

The purified BruN and its mutants were digested with thrombin to remove the His-tag and were concentrated to 18–20 mg/mL for crystallization using sitting drop vapor diffusion method. Protein crystals were screened by commercial crystallization kits with PEGRx, PEGRx2, Crystal Screen, Crystal Screen 2, and Morpheus. Technically, 0.35 μ L protein and 0.35 μ L reservoir solution were mixed in MRC-2Drops 96-well plates. The crystallization drops were incubated at 22°C. Finally, the protein crystal of BruN^{N441M} was obtained after a 2-day incubation in the reservoir solution containing 0.06 M magnesium chloride hexahydrate, 0.06 M calcium chloride dehydrate, 0.1 M imidazole and MES (2-(N-morpholino)ethanesulfonic acid monohydrate) (pH 6.5), 20% v/v ethylene glycol, and 10% w/v PEG 8000.

16. Data collection and refinement

The X-ray data of BruN^{N441M} was collected on the BL18U1 beamline at the Shanghai Synchrotron Radiation Facility (SSRF). The diffraction image was processed with Mosflm. The structure was solved by molecular replacement implemented in Phaser with BTG13 crystal structure (PDB ID code 7Y3W) as the search model. The model produced from molecular replacement was used as the starting model for Phenix Autobuild. The model was manually built in Coot and refined by Phenix refinement. The coordinates for the model of BruN^{N441M} has been deposited in the Protein Data Bank (PDB), <https://www.rcsb.org>, with accession number 8YXS.

17. Isolation of monodictyphenone (4a) and emodinic acid

AO-*brumN* co-transformant cultured on DPY agar plate was inoculated in 400 mL of CDM medium for 2 days at 28°C with 130 rpm agitation. Then the culture liquid as inoculating seed was transferred into each 1000 mL Erlenmeyer flask containing 400 mL of CDM medium, with 25 flasks in total. After another 2 days cultivation, 5 mg of chrysophanol (**2**) dissolved in DMSO was added into each flask, followed by the incubation of an additional 4 days. The fermentation broth obtained through filtering with gauze was extracted with ethyl acetate twice and concentrated *in vacuo*. The crude extract was separated by MPLC (medium performance liquid chromatography) over the ODS (octadecylsilyl) column, which was eluted with a MeOH/H₂O gradient (10:90 → 100:0, v/v) to yield five fractions (F1–F5). Subsequent LC-MS analysis indicated that F3 contained the target product and was further purified by semi-preparative HPLC on an Agilent 1260 Eclipse XDB-C18 column (250 × 9.4 mm, 5 μ m) with a MeOH-H₂O mixture (35:65, v/v, 2 mL/min) to yield monodictyphenone (**4a**) (5 mg, R_t = 12 min).

AO was fermented in exposure to **2** on a larger scale as mentioned above, and the extract derived therefrom was separated by MPLC on an ODS column. The 50:50 MeOH-H₂O eluted fraction containing the wanted compound was purified through semi-preparative HPLC with 40% aqueous acetonitrile containing 0.1% HCOOH to obtain emodin acid (~1.7 mg, R_t = 16.3 min).

18. Generation of cephalanone F (**4b**) from chrysophanol (**2**)

In the presence of NADPH, chrysophanol (**2**) was exposed to BruM and BTG13 in a scaled-up manner (see “*in vitro* enzymatic reaction”). The reaction mixture was purified through semi-preparative HPLC with 35% aqueous acetonitrile containing 0.1% HCOOH to give cephalanone F (**4b**) (~1.6 mg, R_t = 18.7 min).

19. Production of 11-hydroxy monodictyphenone (**5a**) from aloe emodin (**5**)

Aloe emodin (**5**) was subjected to the cleavage by the BruMN co-catalysis in the presence of NADPH in a scaled-up manner as described in the “*in vitro* enzymatic reaction” section. The reaction mixture was purified by semi-preparative HPLC with 17% aqueous acetonitrile containing 0.1% HCOOH to afford 11-hydroxy monodictyphenone (**5a**) (~2.4 mg, R_t = 31.7 min).

20. Chemical capture of chrysophanol hydroquinone (**3**) tautomers

Chrysophanol (**2**, 100 mg) was dissolved in MeCN (80 mL) and added to 2.4 g of K₂CO₃ and 0.3 mL of Me₂SO₄ under the protection of nitrogen atmosphere at room temperature, the mixture was heated by reflux for 5h. After removal of the solvent under reduced pressure, the residue was suspended in H₂O and then partitioned with CH₂Cl₂. The organic phase was dried over MgSO₄ and concentrated *in vacuo* and subjected to Si gel Column Chromatography, eluting with a hexane-EtOAc (1:1) system to yield compound **9** on the basis of TLC analysis. Compound **9** (100 mg) obtained was dissolved in 32 mL of THF and added to 25 mg of tetrabutylammonium bromide as a phase-transfer catalyst, then a solution of Na₂S₂O₄ (300 mg) in H₂O (3 mL) was added under the protection of nitrogen atmosphere at room temperature. The mixture was stirring for 15 min, followed by adding 6 N KOH (1 mL). After stirring for further 5 min, Me₂SO₄ (0.5 mL, 5.3 mmol) was added. Subsequently, the mixture was stirred at the room temperature for 12 h and concentrated under reduced pressure. The residue was successively added to H₂O to suspend and CH₂Cl₂ to extract. Finally, the organic phase was dried over MgSO₄ and concentrated *in vacuo* and for the further purification through semi-preparative HPLC with MeCN-H₂O (85:15, *V/V*, 2 mL/min) to afford compound **12** (2.0 mg, R_t = 22 min) (Figure S22).

21. Theoretical simulation

For the interaction exploration of **3a** and **3b** with BruN, BruN^{N441M} and BTG13, firstly, considering the diversity of **3a** and **3b**'s conformations, these two isomers were geometrically optimized using density functional theory (DFT) method at B3LYP/6-31+G* level with Gaussian16 package, eight conformations (**3a1**, **3a2**, **3a3**, **3a4**; **3b1**, **3b2**, **3b3**, **3b4**) were generated with the vibration frequencies verification. The relative energies of the each conformations were calculated by their Hartree Fork energies with zero - point correction to that of **3a1**.

Then, these eight conformations were used for further evaluation of their binding conformations and affinity to the three enzymes with Surflex - dock package distributed within SYBYL suite. Here, the structure of BruN^{N441M} was the crystallized one in the context (PDB ID: 8YXS), while the 3D structure of BruN was derived from the template of BruN^{N441M} with the mutation of Met441 to Asn441 using Protein Composition Tool, and the crystal structure of BTG13 was extracted from RCSB Protein Data Bank (RCSB PDB) database (PDB ID: 7Y3W). With charge calculated and hydrogens added for the receptors, the eight optimized ligands were docked into the protomol sites of the three enzymes. The ChemScore function was used to assess the binding free energy ($\Delta G_{binding}$, kJ/mol) of the putative binding poses generated by Surflex - dock, with terms for hydrogen bonding, metal - ligand interaction, lipophilic contact, and rational entropy and intercept term included. This function proved to perform well for the evaluation of the binding interaction between metal-contained enzymes and ligands.

Molecular docking of chrysophanol hydroquinone (**3**) with BruN (Alphafold3 modeled)¹⁷ was performed using the same method as mentioned above.

Table S1. Annotation of the *bru* cluster in the *A. brunneoviolaceus* genome.

Gene	Size (aa)	Predicted function	Protein homolog, Origin	Identity (%)	Accession number
<i>bruA</i>	181	Probable hydrolase	R7, <i>Phoma</i> sp. MF5453	32	PP586160
<i>bruB</i>	747	Reducing polyketide synthase	RD-PKS F, <i>Alternaria solani</i>	33	PP586161
<i>bruC</i>	426	transcriptional coactivator	AgnL9, <i>Paecilomyces variotii</i>	56	PP586162
<i>bruD</i>	414	transcription factor	AgnL10, <i>Paecilomyces variotii</i>	31	PP586163
<i>bruE</i>	309	Methyltransferase	AacuQ, <i>Aspergillus aculeatus</i> ATCC 16872	95	PP586145
<i>bruF</i>	145	Monooxygenase	AacuP, <i>Aspergillus aculeatus</i> ATCC 16872	97	PP586146
<i>bruG</i>	153	Monooxygenase	AacuO, <i>Aspergillus aculeatus</i> ATCC 16872	93	PP586147
<i>bruH</i>	265	Short chain dehydrogenase	AgnL6, <i>Paecilomyces variotii</i>	89	PP586148
<i>bruI</i>	312	thioesterase	AacuM, <i>Aspergillus aculeatus</i> ATCC 16872	98	PP586149
<i>bruJ</i>	1782	Non-reducing polyketide synthase	AacuL, <i>Aspergillus aculeatus</i> ATCC 16872	96	PP586150
<i>bruK</i>	265	Dehydratase	AgnL8, <i>Paecilomyces variotii</i>	74	PP586151
<i>bruL</i>	404	Heat shock protein	AacuJ, <i>Aspergillus aculeatus</i> ATCC 16872	88	PP586152
<i>bruM</i>	391	Oxidoreductase	AgnL4, <i>Paecilomyces variotii</i>	76	PP586153
<i>bruN</i>	456	Non-heme iron dioxygenase	CPUR_05427, <i>Claviceps purpurea</i>	64	PP586154
<i>bruO</i>	183	Decarboxylase	ClaH, <i>Cladosporium fulvum</i>	69	PP586155
<i>bruP</i>	266	Short chain dehydrogenase/reductase	AacuF, <i>Aspergillus aculeatus</i> ATCC 16872	92	PP586156
<i>bruQ</i>	519	Cytochrome P450 monooxygenase	AacuE, <i>Aspergillus aculeatus</i> ATCC 16872	95	PP586157
<i>bruR</i>	287	Short chain dehydrogenase/reductase	AacuD, <i>Aspergillus aculeatus</i> ATCC 16872	94	PP586158
<i>bruS</i>	514	FAD-dependent monooxygenase	AacuC, <i>Aspergillus aculeatus</i> ATCC 16872	97	PP586159

Table S2. Functional comparison of proteins encoded by the *bru*, *nsr*, *agn*, *sec*, and *dmx* gene clusters.

<i>bru</i>	Predicted function	<i>Nsr</i> , % id	<i>Agn</i> , % id	<i>sec</i> , % id	<i>Dmx</i> , % id
<i>bruA</i>	Probable hydrolase	–	–	–	–
<i>bruB</i>	Reducing polyketide synthase	–	–	–	–
<i>bruC</i>	coactivator	NsrH, 39	AgnL9, 56	05432, 38	
<i>bruD</i>	Transcription factor	NsrA, 30	AgnL10, 31	05433, 28	R14, 27
<i>bruE</i>	Methyltransferase	NsrG, 48	–	05424, 58	–
<i>bruF</i>	Monooxygenase	NsrQ, 68	–	05417, 51	R10, 48
<i>bruG</i>	Monooxygenase	–	AgnL5, 72	05425, 40	R10, 48
<i>bruH</i>	Short chain dehydrogenase	NsrJ, 67	AgnL6, 89	05429, 73	R18, 71
<i>bruI</i>	Thioesterase	NsrC, 65	AgnL7, 81	05436, 64	R1, 64
<i>bruJ</i>	Non-reducing polyketide synthase	NsrB, 58	AgnPKS, 63	05437, 57	DmxPks, 62
<i>bruK</i>	Dehydratase	NsrI, 52	AgnL8, 74	05428, 53	R17, 58
<i>bruL</i>	Heat shock protein	–	–	–	–
<i>bruM</i>	Oxidoreductase	NsrR, 58	AgnL4, 76	05430, 55	R7, 62
<i>bruN</i>	Baeyer-Villiger oxidase	NsrF, 47	AgnL3, 58	05427, 64	R6, 61
<i>bruO</i>	Decarboxylase	NsrE, 59	AgnL1, 67	05434, 69	R15, 64
<i>bruP</i>	Short chain dehydrogenase	NsrO, 24	–	–	–
<i>bruQ</i>	Cytochrome P450 monooxygenase	NsrP, 48	–	05419, 48	R5, 45
<i>bruR</i>	Short chain dehydrogenase	NsrO, 61	–	05418, 56	R3, 65
<i>bruS</i>	FAD-dependent monooxygenase	NsrK, 58	–	05423, 68	R9, 56

Table S3. Primers used in this study.

Primer	Sequence (5' to 3')
For <i>bruN</i> deletion	
U- <i>bruN</i> -F	GCTCCGAATTCGAGCTCGGTACCgtggaatgaggagaggagaatg
U- <i>bruN</i> -R	CTCCTTCAATATCATCTTCTGaagtttgtaattttacggct
<i>hph1</i> -F	CAGAAGATGATATTGAAGGAG
<i>hph1</i> -R	GCTACTACAGATCCCCGGGTACCAGCGGATTCCTCAGTCTCGTA
D- <i>bruN</i> -F	ATCCTTCTTTCTAGAGGATCCgatctgaggttcagcgtgac
D- <i>bruN</i> -R	GCTACTACAGATCCCCGGGTACCgcgcgacatcttacagtcag
<i>hph2</i> -F	GCTCCGAATTCGAGCTCGGTACCAGACCTGCCTGAAACCGAACT
<i>hph2</i> -R	GGATCCTCTAGAAAGAAGGAT
<i>bruN</i> -A-F	tgaggagaggagaatgggtgag
<i>bruN</i> -A-R	TTCCTCAGTCTCGTAGGTCTCTT
<i>bruN</i> -B-F	TGAAACCGAACTGCCCGCTGTTC
<i>bruN</i> -B-R	catcttacagtcacccgcac
For verification of Δ<i>bruN</i>	
Diag- <i>bruN</i> -F	tcgaacagccggctgatgtg
Diag- <i>bruN</i> -R	gcatagccccagtgtagtt
Diag- <i>hph</i> -F	GAAGAGAAGAATAGCTTAGCAGAGC
For heterologous expression in <i>A. oryzae</i>	
pTAex3- <i>bruM</i> -F	TCCGAATTCGAGCTCGGTACCatgtcggacatcctaaccgccg
pTAex3- <i>bruM</i> -R	TACTACAGATCCCCGGGTACCctagctaggcccgtagatgg
pTAex3- <i>bruN</i> -F	CCACAGCAAGCTCCGAATTCatgggctccaccgcaaccgcaac
pTAex3- <i>bruN</i> -R	TACTACAGATCCCCGGGTACCctaagcaagatccggccggatcttcca
InF-pBARI- <i>SmaI</i> -F	CTAGAGGATCCCCGGGTCCAATCTTCAAGAGCAGAA
InF-pBARI- <i>SmaI</i> -R	GAGCTCGGTACCCGGGGATACATGAGCTTCGGTGAT
For protein expression in <i>E. coli</i> BL21 (DE3)	
pET28a- <i>bruN</i> -F	GGTGCCGCGCGGCAGCCATATGggctccaccgcaaccgcaac
pET28a- <i>bruN</i> -R	GCTCGAGTGCGGCCGCAAGCTTctaagcaagatccggccggatcttc
pET28a- <i>bruM</i> -F	GGTGCCGCGCGGCAGCCATATGtcggacatcctaaccgccga
pET28a- <i>bruM</i> -R	GCTCGAGTGCGGCCGCAAGCTTctagctaggcccgtagat
pET28a- <i>BTG13</i> -F	GGTGCCGCGCGGCAGCCATATGACAGTCCTTGCCACTTCCAG
pET28a- <i>BTG13</i> -R	GCTCGAGTGCGGCCGCAAGCTTCTAAGCCGCTGGTAACGAGT
For single-site mutation in BruN	
<i>bruN</i> -H66F-F	acaaccacatcgcgTTctcgatcctgacctgcctgg
<i>bruN</i> -H66F-R	agAAcgcgatgtggttggtggcccccggctcgc
<i>bruN</i> -H66K-F	atcgcgAAGtcgatcctgacctgcctggcgct
<i>bruN</i> -H66K-R	aggatcgaCTTcgcgatgtggttggtggcccg
<i>bruN</i> -H166F-F	ctacTTcccggatccacctggggctggggat
<i>bruN</i> -H166F-R	tggatcaccgggAAgtaggcgcctcgtacagc
<i>bruN</i> -H308F-F	ctacatgTTaccctcaccagctcgctcttctt
<i>bruN</i> -H308F-R	gtgagggtgAAcatgtagaagaagtcgatcttgcg

<i>bruN</i> -H386F-F	ggTTgtggcgaagatgatccgcgctgaaga
<i>bruN</i> -H386F-R	tcatcttcgccacaAAcccgtcgtcgtcctt
<i>bruN</i> -K389Y-F	tgtggcgTATatgatccgcgctgaagaacg
<i>bruN</i> -K389Y-R	ggatcatATAcgccacatgcccgctcgtcgtc
<i>bruN</i> -T311V-F	tcGTcagctcgtcttcttcagcgtgctcatcc
<i>bruN</i> -T311V-R	agaagagcgcgctgACgaggggtgcatgtagaagaagtcg
<i>bruN</i> -F304A-F	agatcgacGCcttctacatgcacaccctcacca
<i>bruN</i> -F304A-R	tgtagaagGCgtcgtatcttgcttgccggcgg
<i>bruN</i> -F305A-F	atcgacttcGCctacatgcacaccctcaccagc
<i>bruN</i> -F305A-R	catgtagGCgaagtcgatcttgcttgccggcc
<i>bruN</i> -H61F-F	cTTcaaccacatcgcgcactcgtcctgacctg
<i>bruN</i> -H61F-R	tgcgcgatgtggtgAAgcccggcgtcgcggaa
<i>bruN</i> -H63F-F	acaacTTcatcgcgcactcgtcctgacctgcc
<i>bruN</i> -H63F-R	agtgcgcgatgAAGttgtggccccggctgc
<i>bruN</i> -R56E-F	atgttcttcGAGgaccggggccacaacca
<i>bruN</i> -R56E-R	cggtcCTCgaagaacatgtgccattcctcgtg
<i>bruN</i> -F55W-F	aatggcacatgttctGGcgcgaccggggccac
<i>bruN</i> -F55W-R	gCCagaacatgtccattcctcgtggttcttct
<i>bruN</i> -R58D-F	tgttctccgcgacGACgcgggccacaaccacatc
<i>bruN</i> -R58D-R	GTCgtcgcggaagaacatgtgccattcctcgt
<i>bruN</i> -R58V-F	atgttctccgcgacGTggcgggccacaaccacat
<i>bruN</i> -R58V-R	cACgtcgcggaagaacatgtgccattcctcgtg
<i>bruN</i> -A59G-F	gGgggccacaaccacatcgcgcactcgtcct
<i>bruN</i> -A59G-R	atgtggttggtggcccCcccggtcgcggaagaaca
<i>bruN</i> -I91H-F	acggggtgggcCAccagcggccgatcccggcgg
<i>bruN</i> -I91H-R	gctggTGgcccaccccgctcgtcgtaggcgcgct
<i>bruN</i> -A164L-F	tacgagggcCTctaccaccgggtgatccacctg
<i>bruN</i> -A164L-R	gtggtagAGgccctcgtacagccgcgagcat
<i>bruN</i> -F243G-F	gacGGAaggcaacaagatgcgcgacggcgtcgt
<i>bruN</i> -F243G-R	atcttgttgccTCCgtcctcccagcgggggc
<i>bruN</i> -G244P-F	aggacttcCCaacaagatgcgcgacggcgtcgc
<i>bruN</i> -G244P-R	tcttgttgGGAagtcctcccagcggggcgg
<i>bruN</i> -N245V-F	acttcggcGTcaagatgcgcgacggcgtcgtcgc
<i>bruN</i> -N245V-R	gcatcttgACgccgaagtctcccagcggggg
<i>bruN</i> -N245A-F	acttcggcGCcaagatgcgcgacggcgtcgtcgc
<i>bruN</i> -N245A-R	gcatcttgGCgccgaagtctcccagcggggg
<i>bruN</i> -K246R-F	acttcggcaacCGTatgcgcgacggcgtcgtc
<i>bruN</i> -K246R-R	catACGgttgccaagtcctcccagcggggg
<i>bruN</i> -M247V-F	ttcggcaacaagGTTcgcgacggcgtcgtcggc
<i>bruN</i> -M247V-R	cgAACcttgttgccaagtcctcccagcggcg
<i>bruN</i> -V347A-F	tggcctggtacgtggCAagcgggtccgagcgtg
<i>bruN</i> -V347A-R	tTGccacgtaccaggccaaatccagcggccct
<i>bruN</i> -T435I-F	gcccaTTgaccagaagttgtgaattttacggg

<i>bruN</i> -T435I-R	aacttctggtcAAtgggccagtccttggctgtg
<i>bruN</i> -D436P-F	cCCcagaagtttTgaattttacgggcttga
<i>bruN</i> -D436P-R	ttcacaacttctggGGggtgggccagtccttggtc
<i>bruN</i> -V440I-F	ccgaccagaagtttATCaattttacgggcttTgatatggg
<i>bruN</i> -V440I-R	GATaaacttctggtcggtgggccagtccttgg
<i>bruN</i> -N441M-F	gtttgtgaTGtttacgggcttTgatatggggtg
<i>bruN</i> -N441M-R	cccgtaaaCATcacaacttctggtcggtgggc
<i>bruN</i> -N441W-F	gtttgtgTGGtttacgggcttTgatatggggt
<i>bruN</i> -N441W-R	ccgtaaCCAcacaaacttctggtcggtgggc
<i>bruN</i> -F442G-F	ttgtgaatGGtacgggcttTgatatggggtgga
<i>bruN</i> -F442G-R	agcccgtaccattcacaacttctggtcggtgg
<i>bruN</i> -R452V-F	aagatcGTgccgatcttTcttagAAGCTTGCG
<i>bruN</i> -R452V-R	aagatccggcACgatcttccacccatatacaagc
<i>bruN</i> -V347F-F	ttggcctggtacgtgTtcagcgggtccgccgagc
<i>bruN</i> -V347F-R	aAcacgtaccaggccaatcca
<i>bruN</i> -V347L-F	ttggcctggtacgtgCtcagcgggtccgccgagc
<i>bruN</i> -V347L-R	aGcacgtaccaggccaatcca
<i>bruN</i> -V347I-F	ttggcctggtacgtgAtcagcgggtccgccgagc
<i>bruN</i> -V347I-R	aTcacgtaccaggccaatcca
For the saturation mutation of N441 site in BruN	
<i>bruN</i> -N441NNK-F	gtttgtgNNKtttacgggcttTgatatggggtg
<i>bruN</i> -N441NNK-R	cccgtaaaNNKcacaacttctggtcggtgggc
For parts of double-sites mutation in BruN	
<i>bruN</i> -N441M/D436P-F	CCcagaagtttTgaTGtttacgggcttTgatatgggg
<i>bruN</i> -N441M/D436P-R	CATcacaacttctggGGggtgggccagtccttggtc
<i>bruN</i> -N441M/V440I-F	gtttATCaTGtttacgggcttTgatatgggg
<i>bruN</i> -N441M/V440I-R	cccgtaaaCATGATaaacttctggtcggtgggcc
<i>bruN</i> -N441M/F442G-F	agtttTgaTGGGtacgggcttTgatatggggtg
<i>bruN</i> -N441M/F442G-R	ccgtaCCCATcacaacttctggtcggtgg
<i>bruN</i> -N441W/D436P-F	CCcagaagtttTgTGGtttacgggcttTgatatgggg
<i>bruN</i> -N441W/D436P-R	CCAcacaaacttctggGGggtgggccagtccttggtc
<i>bruN</i> -N441W/D436E-F	cccaccgaAcagaagtttTgTGtttacggg
<i>bruN</i> -N441W/D436E-R	aacttctgTtcggtgggccagtccttggctgt
<i>bruN</i> -N441W/T435I-F	gaccagaagtttTgTGtttacgggcttTgatatgggg
<i>bruN</i> -N441W/T435I-R	CCAcacaaacttctggtcAAtgggccagtccttggctg
<i>bruN</i> -N441W/V440I-F	gtttATCTGGtttacgggcttTgatatgggg
<i>bruN</i> -N441W/V440I-R	cccgtaaaCCAGATaaacttctggtcggtgggcc
<i>bruN</i> -N441W/F442G-F	agtttTgTGGGtacgggcttTgatatggggtg
<i>bruN</i> -N441W/F442G-R	cgtaCCCCAcacaacttctggtcggtggg
<i>bruN</i> -F55W/R58D-F	tgttctGGcgcgacGACcgggccacaaccacatc
<i>bruN</i> -F55W/R58D-R	GTCgtcgcgCCagaacatgtgccattcctcgtg
<i>bruN</i> -F55W/R58V-F	atgttctGGcgcgacGTggcgggccacaaccacat
<i>bruN</i> -F55W/R58V-R	cACgtcgcgCCagaacatgtgccattcctcgtg

<i>bruN</i> -N41F/T435I-F	TgaccagaagtttgTtTtttacgggctttgatatgggg
<i>bruN</i> -N41F/T435I-R	AcacaaactctggtcAAtgggccagtccttggtcg
<i>bruN</i> -N41F/T435D-F	GAcgaccagaagtttgTtTtttacgggctttgatatgggg
<i>bruN</i> -N41F/T435D-R	cacaaactctggtcgTCgggccagtccttggtcgt
<i>bruN</i> -N41F/D436P-F	CCcagaagtttgTtTtttacgggctttgatatgggg
<i>bruN</i> -N41F/D436P-R	AAcacaaactctggGGggtgggccagtccttggtc
<i>bruN</i> -N41F/D436E-F	gaAcagaagtttgTtTtttacgggctttgatatgggg
<i>bruN</i> -N41F/D436E-R	AAcacaaactctgTtcggtgggccagtccttg
<i>bruN</i> -N41F/D436Q-F	CaGcagaagtttgTtTtttacgggctttgatatgggg
<i>bruN</i> -N41F/D436Q-R	AAcacaaactctgCtGggtgggccagtccttggtc
<i>bruN</i> -N41F/Q437NNK-F	cgacNNKaagtttgTtTtttacgggctttgatatgggg
<i>bruN</i> -N41F/Q437NNK-R	AAcacaaactNNKgtcgtgggccagtcctt
<i>bruN</i> -N41F/V440I-F	ttATCTTtttacgggctttgatatgggg
<i>bruN</i> -N41F/V440I-R	gcccgtaaaaAAGATaaactctggtcggtggcc
<i>bruN</i> -N41F/F442G-F	tttgTtTtGGtacgggctttgatatgggggtg
<i>bruN</i> -N41F/F442G-R	cccgtACCaaAcacaaactctggtcggtggg
For parts of multiple-sites mutation in BruN	
<i>bruN-AA^a</i> -F	CCcagaagtttATCTGGGGtacgggctttgatatgggggtg
<i>bruN-AA^a</i> -R	CCAGATaaactctggGGAAtgggccagtccttggtcg
<i>bruN-BB^b</i> -F	TCCcGCgaagtGGATCaTGGGtacgggctttgatatgggggtg
<i>bruN-BB^b</i> -R	AtGATCCacttcGCgGGAAtgggccagtccttggtcg
<i>bruN-CC^c</i> -F	acGGACCcGTcCGTgtgCGcgcggcgtcgtcg
<i>bruN-CC^c</i> -R	caCACGgACgGGTCCgtcctcccagcgggggc
<i>bruN</i> -N41F/Q437A/V440I-F	cgacGCgaagtttATCTTtttacgggctttgatatgggg
<i>bruN</i> -N41F/Q437A/V440I-R	AAGATaaacttcGCgtcggtgggccagtcctt
For single-site mutation in BTG13	
<i>BTG13</i> -M427N-F	AATGGATCAatGGCGCTGGTTACGATTTCTTAT
<i>BTG13</i> -M427N-R	CAGCGCCatTGATCCATTTGGCGGGAATCGGAA
<i>BTG13</i> -M427F-F	ATGGATCtttGGCGCTGGTTACGATTTCTTAT
<i>BTG13</i> -M427F-R	CAGCGCCaaaGATCCATTTGGCGGGAATCGGAA
<i>BTG13</i> -M427V-F	AATGGATCgTGGCGCTGGTTACGATTTCTTA
<i>BTG13</i> -M427V-R	AGCGCCAcGATCCATTTGGCGGGAATCGGAA
<i>BTG13</i> -M427P-F	AAATGGATCccGGGCGCTGGTTACGATTTCTTA
<i>BTG13</i> -M427P-R	AGCGCCCggGATCCATTTGGCGGGAATCGGAAG

^aAA stands for multiple-sites mutation with T435I/D436P/V440I/N441W/F442G.

^bBB stands for the multiple-sites mutation with T435I/D436P/Q437A/F439W/V440I/N441M/F442G.

^cCC stands for multiple-sites mutation with F243G/G244P/N245V/K246R/M247V.

Table S4. Plasmids constructed for this study.

Plasmid	Inserts	Primer 1	Primer 2	PCR template	Vector
pTAex3- Δ <i>bruN</i> -A	<i>Up-bruN</i>	U- <i>bruN</i> -F	U- <i>bruN</i> -R	gDNA	pTAex3 digested with <i>KpnI</i>
	<i>hph1</i>	<i>hph1</i> -F	<i>hph1</i> -R	pSH75	
pTAex3- Δ <i>bruN</i> -B	<i>hph2</i>	<i>hph2</i> -F	<i>hph2</i> -R	pSH75	pTAex3 digested with <i>KpnI</i>
	<i>Down-bruN</i>	D- <i>bruN</i> -F	D- <i>bruN</i> -R	gDNA	
pTAex3- <i>bruN</i>	<i>bruN</i>	pTAex3- <i>bruN</i> -F	pTAex3- <i>bruN</i> -R	gDNA	pTAex3 digested with <i>KpnI</i>
pTAex3- <i>bruM</i>	<i>bruM</i>	pTAex3- <i>bruM</i> -F	pTAex3- <i>bruM</i> -R	gDNA	pTAex3 digested with <i>KpnI</i>
pBARI- <i>bruM</i>	<i>PamyB-bruM-TamyB</i>	InF-pBARI- <i>SmaI</i> -F	InF-pBARI- <i>SmaI</i> -R	pTAex3- <i>bruM</i>	pBARI digested with <i>SmaI</i>
For constructing plasmids with single-site mutations (marked as SSM) in BruN					
pET28a- <i>bruN</i> -SSM	—	<i>bruN</i> -SSM-F	<i>bruN</i> -SSM-R	pET28a- <i>bruN</i>	—
For constructing plasmids with double-site mutations in BruN					
pET28a- <i>bruN</i> -N441M/D436P	—	<i>bruN</i> -N441M/D436P-F	<i>bruN</i> -N441M/D436P-R	pET28a- <i>bruN</i>	—
pET28a- <i>bruN</i> -N441M/V440I	—	<i>bruN</i> -N441M/V440I-F	<i>bruN</i> -N441M/V440I-R	pET28a- <i>bruN</i>	—
pET28a- <i>bruN</i> -N441M/F442G	—	<i>bruN</i> -N441M/F442G-F	<i>bruN</i> -N441M/F442G-R	pET28a- <i>bruN</i>	—
pET28a- <i>bruN</i> -N441W/D436E	—	<i>bruN</i> -N441W/D436E-F	<i>bruN</i> -N441W/D436E-R	pET28a- <i>bruN</i>	—
pET28a- <i>bruN</i> -N441W/T435I	—	<i>bruN</i> -N441W/T435I-F	<i>bruN</i> -N441W/T435I-R	pET28a- <i>bruN</i>	—
pET28a- <i>bruN</i> -N441W/V440I	—	<i>bruN</i> -N441W/V440I-F	<i>bruN</i> -N441W/V440I-R	pET28a- <i>bruN</i>	—
pET28a- <i>bruN</i> -N441W/F442G	—	<i>bruN</i> -N441W/F442G-F	<i>bruN</i> -N441W/F442G-R	pET28a- <i>bruN</i>	—
pET28a- <i>bruN</i> -N441M/F55W	—	<i>bruN</i> -F55W-F	<i>bruN</i> -F55W-R	pET28a- <i>bruN</i> -N441M	—
pET28a- <i>bruN</i> -N441M/R58V	—	<i>bruN</i> -R58V-F	<i>bruN</i> -R58V-R		—
pET28a- <i>bruN</i> -N441M/R452V	—	<i>bruN</i> -452V-F	<i>bruN</i> -R452V-R		—
pET28a- <i>bruN</i> -N441W/F55W	—	<i>bruN</i> -F55W-F	<i>bruN</i> -F55W-R		—
pET28a- <i>bruN</i> -N441W/R58V	—	<i>bruN</i> -R58V-F	<i>bruN</i> -R58V-R		—
	—	<i>bruN</i> -R58V-F	<i>bruN</i> -R58V-R		—

pET28a- <i>bruN</i> -N441W/A164L	—	<i>bruN</i> -A164L-F	<i>bruN</i> -A164L-R	pET28a- <i>bruN</i> -N441W	—
pET28a- <i>bruN</i> -N441W/F243G	—	<i>bruN</i> -F243G-F	<i>bruN</i> -F243G-R		—
pET28a- <i>bruN</i> -N441W/G244P	—	<i>bruN</i> -G244P-F	<i>bruN</i> -G244P-R		—
pET28a- <i>bruN</i> -N441W/N245V	—	<i>bruN</i> -N245V-F	<i>bruN</i> -N245V-R		—
pET28a- <i>bruN</i> -N441W/V347A	—	<i>bruN</i> -V347A-F	<i>bruN</i> -V347A-R		—
pET28a- <i>bruN</i> -N441W/R452V	—	<i>bruN</i> -R452V-F	<i>bruN</i> -R452V-R		—
pET28a- <i>bruN</i> -N441F/F55W	—	<i>bruN</i> -F55W-F	<i>bruN</i> -F55W-R	pET28a- <i>bruN</i> -N441F	—
pET28a- <i>bruN</i> -N441F/R58V	—	<i>bruN</i> -R58V-F	<i>bruN</i> -R58V-R		—
pET28a- <i>bruN</i> -N441F/I91H	—	<i>bruN</i> -I91H-F	<i>bruN</i> -I91H-R		—
pET28a- <i>bruN</i> -N441F/A164L	—	<i>bruN</i> -A164L-F	<i>bruN</i> -A164L-R		—
pET28a- <i>bruN</i> -N441F/F243G	—	<i>bruN</i> -F243G-F	<i>bruN</i> -F243G-R		—
pET28a- <i>bruN</i> -N441F/G244P	—	<i>bruN</i> -G244P-F	<i>bruN</i> -G244P-R		—
pET28a- <i>bruN</i> -N441F/N245V	—	<i>bruN</i> -N245V-F	<i>bruN</i> -N245V-R		—
pET28a- <i>bruN</i> -N441F/N245A	—	<i>bruN</i> -N245A-F	<i>bruN</i> -N245A-R		—
pET28a- <i>bruN</i> -N441F/K246R	—	<i>bruN</i> -K246R-F	<i>bruN</i> -K246R-R		—
pET28a- <i>bruN</i> -N441F/M247V	—	<i>bruN</i> -M247V-F	<i>bruN</i> -M247V-R		—
pET28a- <i>bruN</i> -N441F/V347A	—	<i>bruN</i> -V347A-F	<i>bruN</i> -V347A-R		—
pET28a- <i>bruN</i> -N441F/R452V	—	<i>bruN</i> -R452V-F	<i>bruN</i> -R452V-R		—
pET28a- <i>bruN</i> -N441F/V347I	—	<i>bruN</i> -V347I-F	<i>bruN</i> -V347I-R		—
pET28a- <i>bruN</i> -N441F/V347L	—	<i>bruN</i> -V347L-F	<i>bruN</i> -V347L-R		—
pET28a- <i>bruN</i> -N441F/V347F	—	<i>bruN</i> -V347F-F	<i>bruN</i> -V347F-R		—
pET28a- <i>bruN</i> -N441F/T435I	—	<i>bruN</i> -N441F/T435I-F	<i>bruN</i> -N441F/T435I-R		pET28a- <i>bruN</i>
pET28a- <i>bruN</i> -N441F/T435D	—	<i>bruN</i> -N441F/T435D-F	<i>bruN</i> -N441F/T435D-R	pET28a- <i>bruN</i>	—
pET28a- <i>bruN</i> -N441F/D436P	—	<i>bruN</i> -N441F/D436P-F	<i>bruN</i> -N441F/D436P-R	pET28a- <i>bruN</i>	—
pET28a- <i>bruN</i> -N441F/D436E	—	<i>bruN</i> -N441F/D436E-F	<i>bruN</i> -N441F/D436E-R	pET28a- <i>bruN</i>	—

pET28a- <i>bruN</i> -N441F/D436Q	–	<i>bruN</i> -N441F/D436Q-F	<i>bruN</i> -N441F/D436Q-R	pET28a- <i>bruN</i>	–
pET28a- <i>bruN</i> -N441F/ Q437NNK	–	<i>bruN</i> -N441F/ Q437NNK-F	<i>bruN</i> -N441F/ Q437NNK-R	pET28a- <i>bruN</i>	–
pET28a- <i>bruN</i> -N441F/V440I	–	<i>bruN</i> -N441F/V440I-F	<i>bruN</i> -N441F/V440I-R	pET28a- <i>bruN</i>	–
pET28a- <i>bruN</i> -N441F/F442G	–	<i>bruN</i> -N441F/F442G-F	<i>bruN</i> -N441F/F442G-R	pET28a- <i>bruN</i>	–
For constructing plasmids with mutiple-site mutations in BruN					
pET28a- <i>bruN</i> -N441W/R452V/F55W		<i>bruN</i> -F55W-F	<i>bruN</i> -F55W-R	pET28a- <i>bruN</i> - N441W/R452V	–
pET28a- <i>bruN</i> -N441W/R452V/R58V		<i>bruN</i> -R58V-F	<i>bruN</i> -R58V-R		–
pET28a- <i>bruN</i> -N441W/R452V/F243G		<i>bruN</i> -F243G-F	<i>bruN</i> -F243G-R		–
pET28a- <i>bruN</i> -N441W/R452V/G244P		<i>bruN</i> -F243G-F	<i>bruN</i> -F243G-R		–
pET28a- <i>bruN</i> -N441W/R452V/N245V		<i>bruN</i> -N245V-F	<i>bruN</i> -N245V-R		–
pET28a- <i>bruN</i> -N441W/R452V/V347A		<i>bruN</i> -V347A-F	<i>bruN</i> -V347A-R		–
pET28a- <i>bruN</i> -N441W/R452V/T435I		<i>bruN</i> -N441W/T435I-F	<i>bruN</i> -N441W/T435I-R	pET28a- <i>bruN</i> -R452V	–
pET28a- <i>bruN</i> -N441W/R452V/D436P		<i>bruN</i> -N441W/D436P-F	<i>bruN</i> -N441W/D436P-R		–
pET28a- <i>bruN</i> -N441W/R452V/V440I		<i>bruN</i> -N441W/V440I-F	<i>bruN</i> -N441W/V440I-R		–
pET28a- <i>bruN</i> -N441W/R452V/F442G		<i>bruN</i> -N441W/F442G-F	<i>bruN</i> -N441W/F442G-R		–
pET28a- <i>bruN</i> -N441M/R452V/V440I		<i>bruN</i> -N441M/V440I-F	<i>bruN</i> -N441M/V440I-R		–
pET28a- <i>bruN</i> -N441M/R452V/F442G		<i>bruN</i> -N441M/F442G-F	<i>bruN</i> -N441M/F442G-R		–
pET28a- <i>bruN</i> -N441F/Q437A/V440I		<i>bruN</i> -N41F/Q437A/ V440I-F	<i>bruN</i> -N41F/Q437A/ V440I-R	pET28a- <i>bruN</i>	–
pET28a- <i>bruN</i> -N441F/Q437A/A164L		<i>bruN</i> -A164L-F	<i>bruN</i> -A164L-R	pET28a- <i>bruN</i> - N441F/Q437A	–
pET28a- <i>bruN</i> -N441F/Q437A/V347L		<i>bruN</i> -V347L-F	<i>bruN</i> -V347L-R		–
pET28a- <i>bruN</i> -N441F/V440I/V347L		<i>bruN</i> -V347L-F	<i>bruN</i> -V347L-R	pET28a- <i>bruN</i> - N441F/V440I	–
pET28a- <i>bruN</i> -AA ^a		<i>bruN</i> -AA-F	<i>bruN</i> -AA-R	pET28a- <i>bruN</i>	–

pET28a- <i>bruN-BB^b</i>	<i>bruN-BB-F</i>	<i>bruN-BB-R</i>		—
pET28a- <i>bruN-AA^a/R452V</i>	<i>bruN-AA-F</i>	<i>bruN-AA-R</i>	pET28a- <i>bruN-AA</i>	
pET28a- <i>bruN-BB^b/R452V</i>	<i>bruN-BB-F</i>	<i>bruN-BB-R</i>	pET28a- <i>bruN-BB</i>	
pET28a- <i>bruN-AA^a/R452V/V347A</i>	<i>bruN-V347A-F</i>	<i>bruN-V347A-R</i>	pET28a- <i>bruN-AA/R452V</i>	
pET28a- <i>bruN-BB^b/R452V/V347A</i>	<i>bruN-V347A-F</i>	<i>bruN-V347A-R</i>	pET28a- <i>bruN-BB/R452V</i>	
pET28a- <i>bruN-AA^a/R452V/V347A/CC^c</i>	<i>bruN-CC-F</i>	<i>bruN-CC-R</i>	pET28a- <i>bruN-AA/R452V/V347A</i>	
pET28a- <i>bruN-BB^b/R452V/V347A/CC^c</i>	<i>bruN-CC-F</i>	<i>bruN-CC-R</i>	pET28a- <i>bruN-BB/R452V/V347A</i>	
pET28a- <i>bruN-AA^a/R452V/V347A/CC^c/F55W/R58V</i>	<i>bruN-F55W/R58V-F</i>	<i>bruN-F55W/R58V-F</i>	pET28a- <i>bruN-AA/R452V/V347A/CC</i>	
pET28a- <i>bruN-BB^b/R452V/V347A/CC^c/F55W/R58D</i>	<i>bruN-F55W/R58D-F</i>	<i>bruN-F55W/R58D-F</i>	pET28a- <i>bruN-BB/R452V/V347A/CC</i>	
pET28a- <i>bruN-AA^a/R452V/V347A/CC^c/F55W/R58V/A164L</i>	<i>bruN-A164L-F</i>	<i>bruN-A164L-F</i>	pET28a- <i>bruN-AA/R452V/V347A/CC/F55W/R58V</i>	
pET28a- <i>bruN-BB^b/R452V/V347A/CC^c/F55W/R58D/I91H</i>	<i>bruN-I91H-F</i>	<i>bruN-I91H-F</i>	pET28a- <i>bruN-BB/R452V/V347A/CC/F55W/R58D</i>	
For constructing plasmids with M427 site mutations in BTG13				
pET28a- <i>BTG13-M427X</i>	—	<i>bruN-M427X-F</i>	<i>bruN-M427X-R</i>	pET28a- <i>BTG13</i>

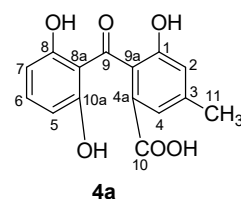
^a*AA* stands for the multiple-sites mutation with T435I/D436P/V440I/N441W/F442G.

^b*BB* stands for the multiple-sites mutation with T435I/D436P/Q437A/F439W/V440I/N441M/F442G.

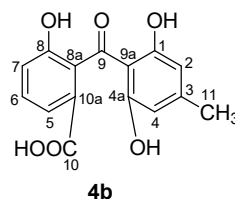
^c*CC* stands for the multiple-sites mutation with F243G/G244P/N245V/K246R/M247V.

Table S5. ^1H (500 MHz) and ^{13}C NMR (125 MHz) data of monodictyphenone (**4a**).¹⁸

position	δ_{H} (<i>J</i> in Hz)	δ_{C}
1		154.0
2	7.30 s	122.2
3		139.4
4	6.91 s	120.7
4a		130.6
5	6.33 d (8.5)	108.0
6	7.21 t (8.5)	136.5
7	6.33 d (8.5)	108.0
8		162.6
8a		113.0
9		202.2
9a		131.7
10		168.3
10a		162.6
11	2.31 s	21.1

**Table S6.** ^1H NMR (500 MHz) data of cephalanone F (**4b**).^{4,19}

position	4b
2	6.18 s
4	6.18 s
5	7.49 d (8.0)
6	7.25 t (8.0)
7	7.10 d (8.0)
11	2.18 s

**Table S7.** ^1H NMR (500 MHz) data of 11-hydroxy monodictyphenone (**5a**) in CD_3OD .²⁰

position	5a
2	7.03 s
4	7.47 s
5	6.28 d (8.0)
6	7.19 t (8.0)
7	6.28 d (8.0)
11	4.60 s

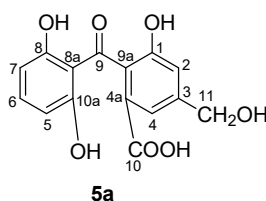
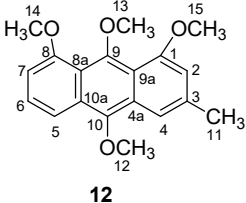


Table S8. ^1H (600 MHz) and ^{13}C NMR (150 MHz) data of **12** in CDCl_3 .²¹

position	δ_{H} (<i>J</i> in Hz)	δ_{C}
1		157.3
2	6.61 s	106.8
3		117.7
4	7.61 s	112.9
4a		135.9
5	7.82 d (8.4)	114.5
6	7.37 t (8.4, 7.8)	125.9
7	6.74 d (7.8)	103.7
8		157.6
8a		118.4
9		151.0
9a		127.7
10		146.6
10a		127.7
11	2.53 s	22.6
12	4.02 s	62.5
13	3.88 s	63.8
14	4.03 s	56.4
15	4.03 s	56.4

**Table S9.** ^1H NMR (500 MHz) data of emodinic acid.²²

position	Emodinic acid
2	6.91 brs
4	6.58 brs
5	6.32 brs
7	6.49 brs
11	2.11 s

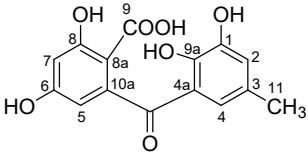


Table S10. X-ray data collection and refinement statistics.

	BruN ^{N441M}
Space group	C1 2 1
Cell dimensions	
No. reflections	53022
a, b, c (Å)	256.99, 109.74, 179.81
α , β , γ (°)	90.00, 93.40, 90.00
Resolution (Å)	179.58-3.62 (3.82-3.62)
R _{merge} (%)	49.1 (139)
I / σ I	3.4 (1.5)
Completeness (%)	100
Redundancy	5.1 (5.2)
R _{work} / R _{free} (%)	28.11 (34.12) / 31.68 (35.48)
B-factors	96.72
Bond lengths (Å)	0.003
Bond angles (°)	0.51
Ligand/ion	5
Water	20

Table S11. Interactivity comparison of substrate tautomers with BruN, BruN^{N441M}, and BTG13.

Interactivities between BruN and tautomers			
Isomers	$\Delta G_{binding}$ (kJ/mol)	Isomers	$\Delta G_{binding}$ (kJ/mol)
3a1	-23.42	3b1	-22.82
3a2	-25.32	3b2	-22.39
3a3	-25.03	3b3	-23.21
3a4	-24.81	3b4	-22.28
Interactivities between BruN ^{N441M} and tautomers			
Isomers	$\Delta G_{binding}$ (kJ/mol)	Isomers	$\Delta G_{binding}$ (kJ/mol)
3a1	-20.99	3b1	--
3a2	--	3b2	-18.00
3a3	-20.33	3b3	-21.84
3a4	-22.20	3b4	--
Interactivities between BTG13 and tautomers			
Isomers	$\Delta G_{binding}$ (kJ/mol)	Isomers	$\Delta G_{binding}$ (kJ/mol)
3a1	--	3b1	-24.34
3a2	-23.37	3b2	-27.34
3a3	-24.86	3b3	-27.22
3a4	--	3b4	-23.74

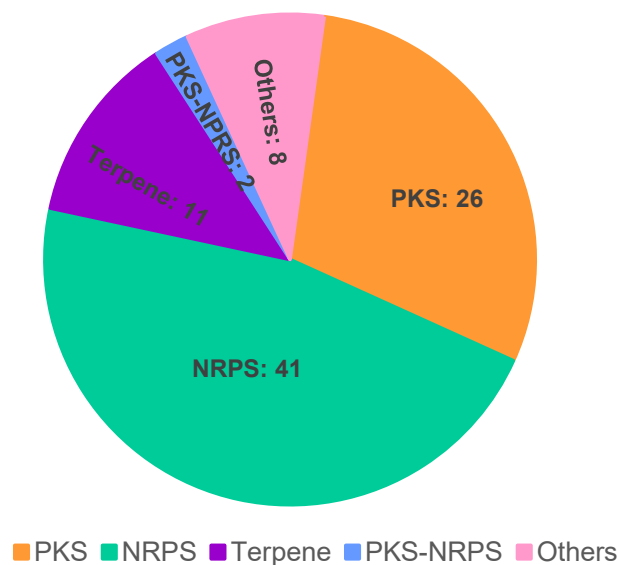


Figure S1. The 88 biosynthetic gene clusters predicted by AntiSMASH (fungal version) in *A. brunneoviolaceus*. PKS: polyketide synthase; NRPS: Non-ribosomal peptide synthetase.

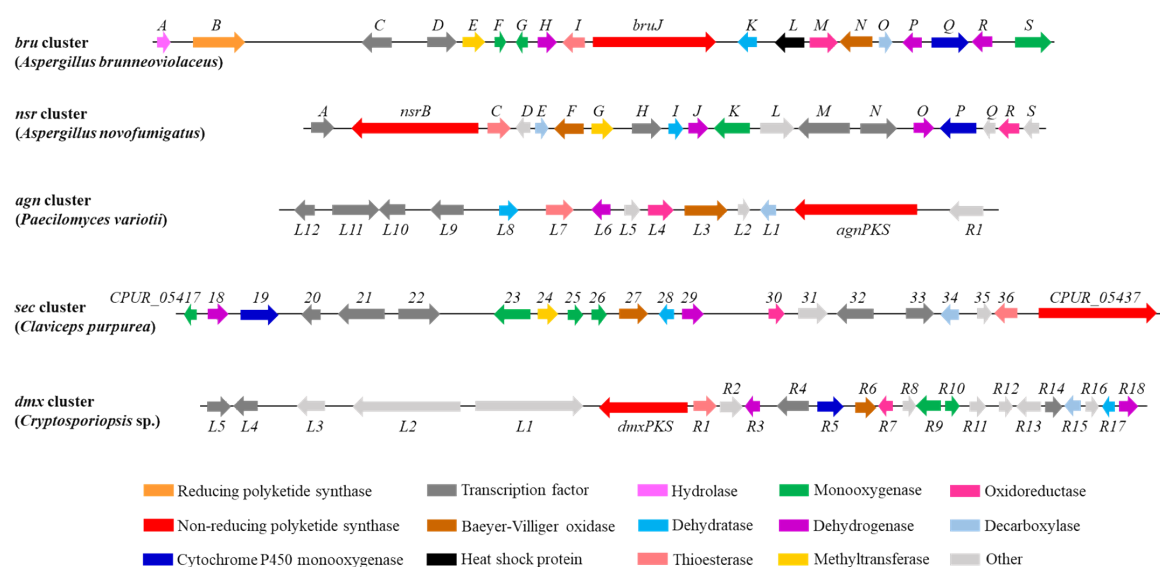


Figure S2. Comparison of the *bru* cluster with its homologues in fungi. Functionally conserved genes are labeled with the same color. The detailed similarity was listed in Table S2.

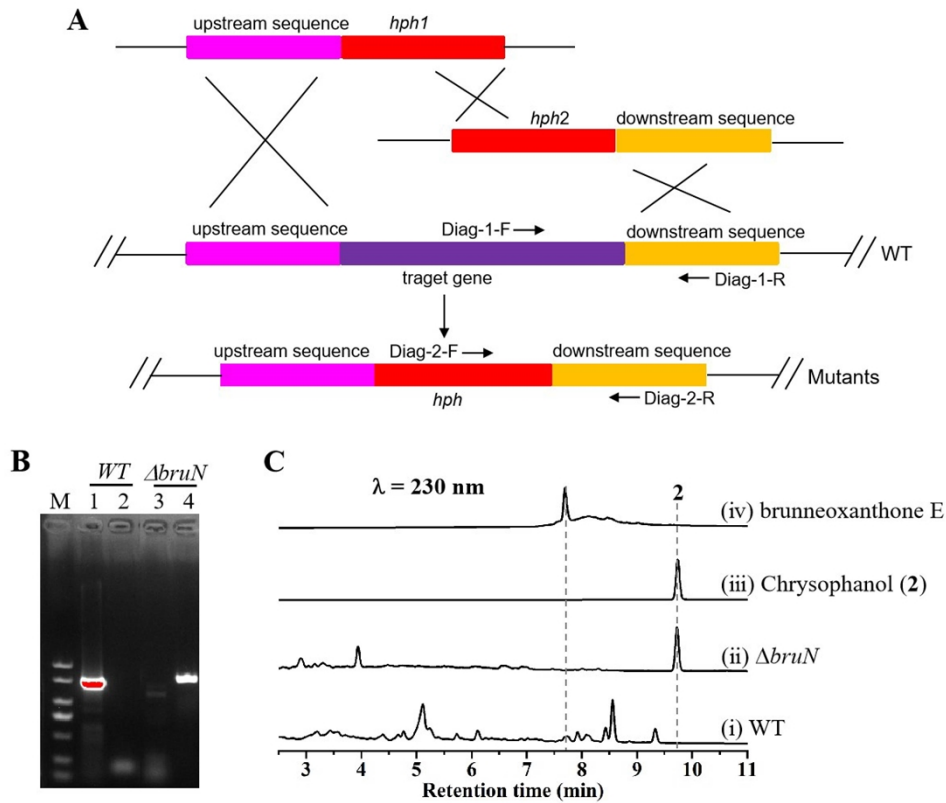


Figure S3. Deletion of the *bruN* gene from the *A. brunneoviolaceus* genome. (A) The scheme of hygromycin-resistance split marker strategy for gene deletion. (B) PCR verification of $\Delta bruN$ mutant: Lane 1, amplified with Diag-1-F/Diag-1-R and WT genome template as control; Lane 2, amplified with Diag-2-F/Diag-2-R and WT genome template as control; Lane 3, amplified with Diag-1-F/Diag-1-R and $\Delta bruN$ genome template; Lane 4, amplified with Diag-2-F/Diag-2-R and $\Delta bruN$ genome template. For the gene knockout mutant of $\Delta bruN$, the expected band in lane 4 was about 1.1 kb, and no band present in lane 3 with equally sized. (C) HPLC analysis of metabolites from wild-type (WT) and mutant strain ($\Delta bruN$) recorded at 230 nm.

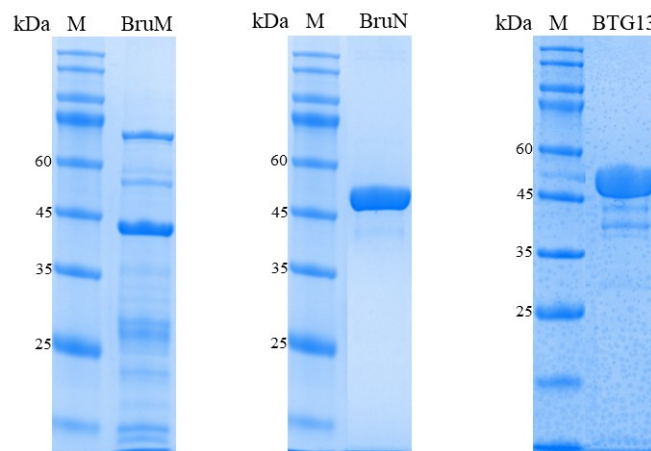


Figure S4. SDS-PAGE analysis of BruM (38.6 kDa), BruN (53.0 kDa), and BTG13 (WAU16873.1, 51.6 kDa).

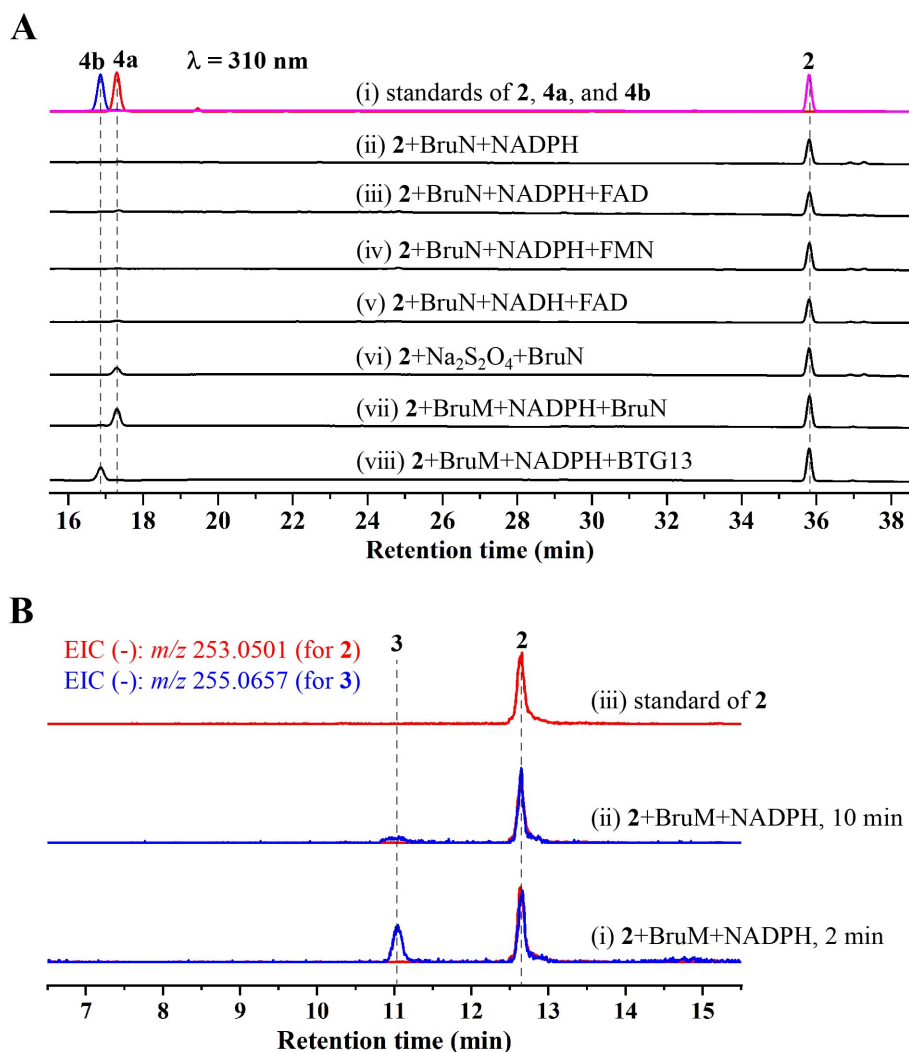


Figure S5. LC-MS assay for the chrysophanol (**2**)-derived products from the *in vitro* enzymatic reactions. (A) HPLC profiles of **2**-derived products in the presence of Na₂S₂O₄, or BruM plus BruN (or BTG13) with NADPH as an electron donor. The LC-MS analysis was performed using the duration-dependent methanol/water (containing 0.1% formic acid) gradients (0→10 min, 5:95→35:65; 10→35 min, 35:65→100:0; 35→40 min, pure methanol). (B) LC-MS detection of **2**-derived products from the *in vitro* assay of BruM in the presence of NADPH with different reaction time. The LC-MS analysis was performed using an acetonitrile/water gradient (0→13 min, 10:90→100:0; 13→18 min, pure acetonitrile).

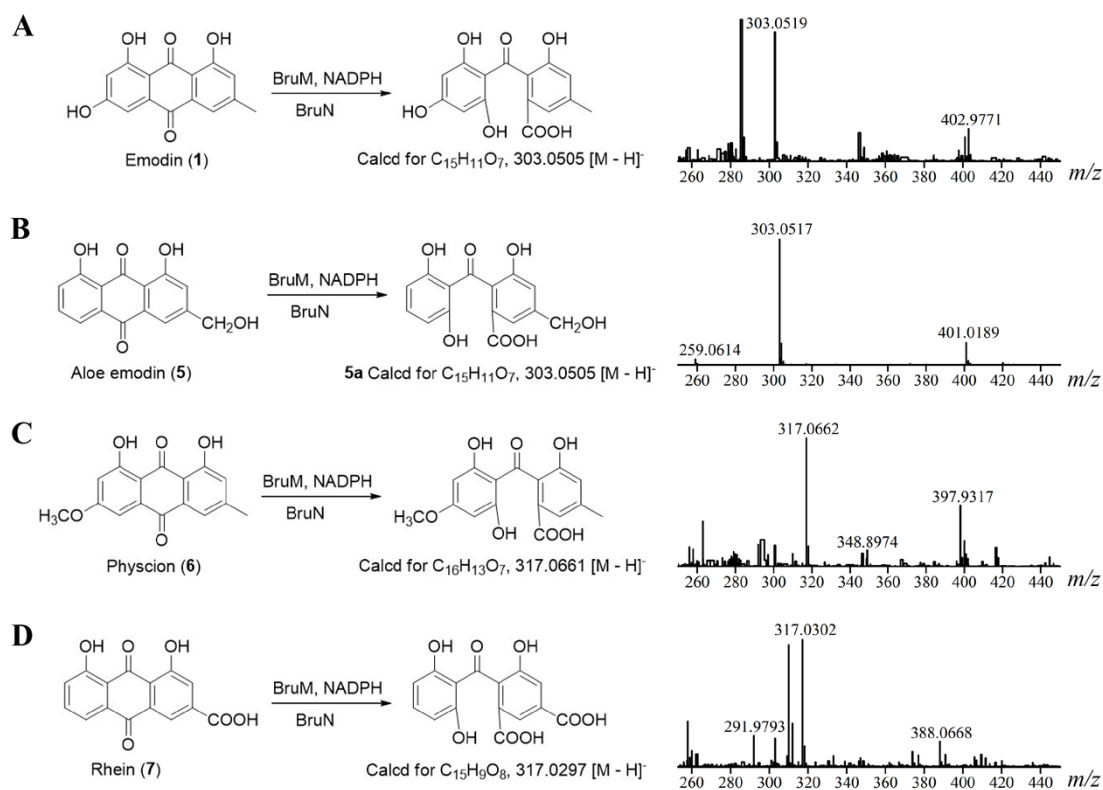


Figure S6. LC-MS analyses (negative ion mode) of ring-opened products of emodin (1), aloe emodin (5), physcion (6), and rhein (7), after individually exposed to BruMN in presence of NADPH.

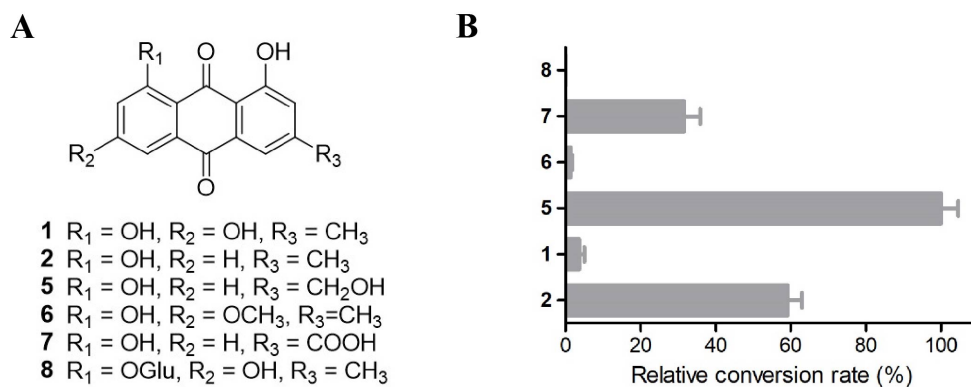


Figure S7. Conversion rate comparison of BruMN catalyzed fission of 1, 2, and 5–7 (see Figure S6).

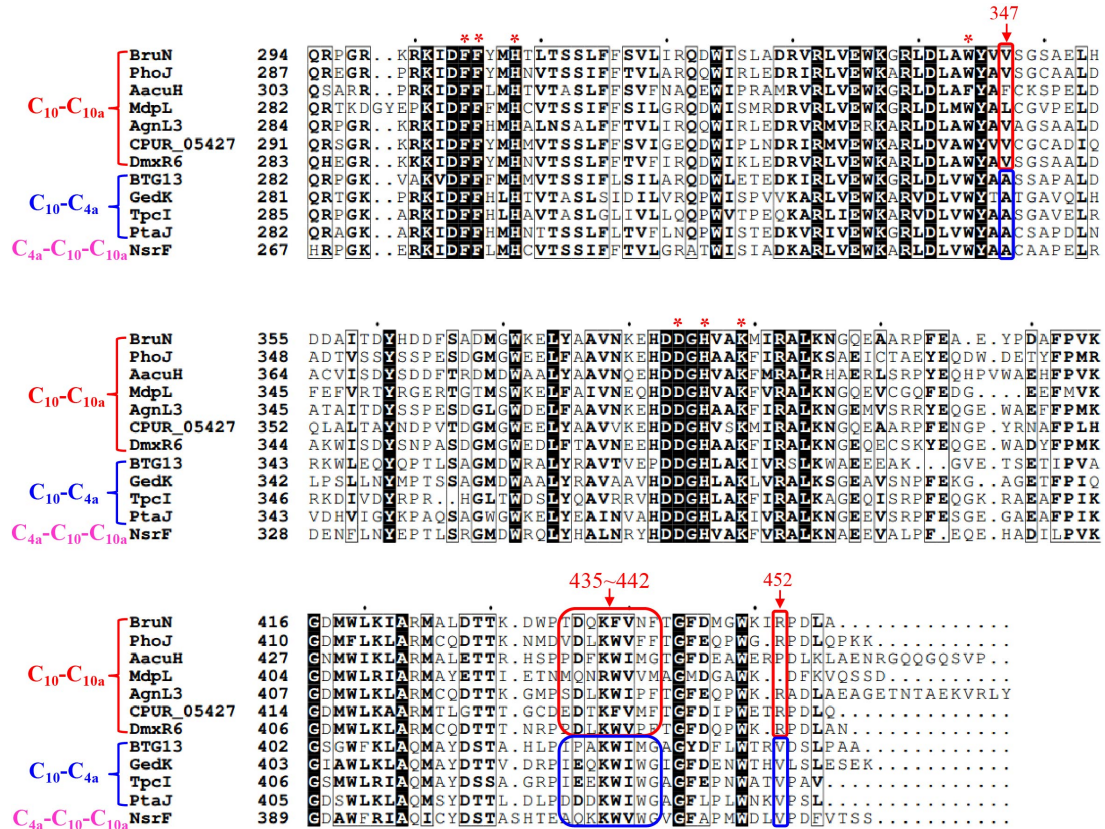


Figure S8. Multiple sequence alignment of BruN with its homologs using ClustalX2.1. The completely conserved residues around the 5Å of substrate are highlighted with red asterisks, according to the molecular docking of substrate **3** with modeled BruN, with the structure predicted by AlphaFold3. Lys389, as one of five residues coordinating to a divalent metal ion of BruN (His63, His166, His308, His386, and Lys389), is also conserved and highlighted with red asterisk. The varied residues around the 5Å of substrate among the curated BruN homologues are compared, with the residue numbers of BruN are indicated. The proteins possessing different pattern of catalyzing C-C bond cleavage are shown. PhoJ (UPG58739.1) from *Diaporthe* sp., AacuH (A0A1L9WLI9.1) from *Aspergillus aculeatus*, MdpL (C8VQ61.1) from *Aspergillus nidulans*, AgnL3 (A0A411PQN8.1) from *Paecilomyces variotii*, CPUR_05427 (M1WG92.1) from *Claviceps purpurea*, DmxR6 (A0A4P8DJZ3.1) from *Cryptosporiopsis* sp., BTG13 (PDB code: 7Y3W, WAU16873.1) from *Cercospora* sp., GedK (Q0CCX5.1) from *Aspergillus terreus*, TpcI (Q4WQY9.1) from *Aspergillus fumigatus*, PtaJ (A0A067XMK8.1) from *Pestalotiopsis fici*, NsrF (A0A2I1C3U2.1) from *Aspergillus novofumigatus*.

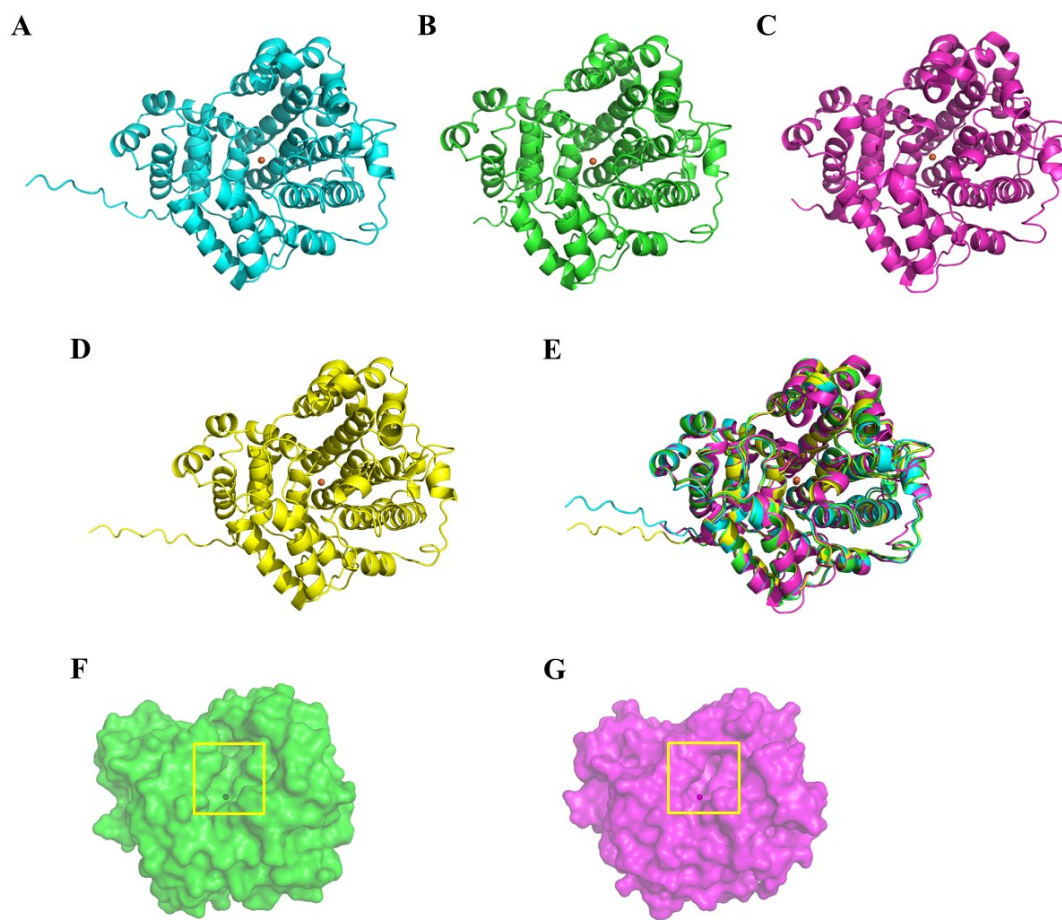


Figure S9. Structural comparison of BruN, BruN^{N441M}, BTG13, and BruN^{N441F/Q437A/V347L}. (A) BruN modeled by AlphaFold3,¹⁷ (B) BruN^{N441M} (PDB: 8YXS), (C) BTG13 (PDB: 7Y3W) reported in ref.⁴, (D) BruN^{N441F/Q437A/V347L} modeled by AlphaFold3,¹⁷ (E) superimposed image of BruN (cyan), BruN^{N441M} (green), BTG13 (magenta), and BruN^{N441F/Q437A/V347L} (yellow). (F and G) surface structures of BruN^{N441M} and BTG13 with substrate binding pocket location marked in yellow rectangle.

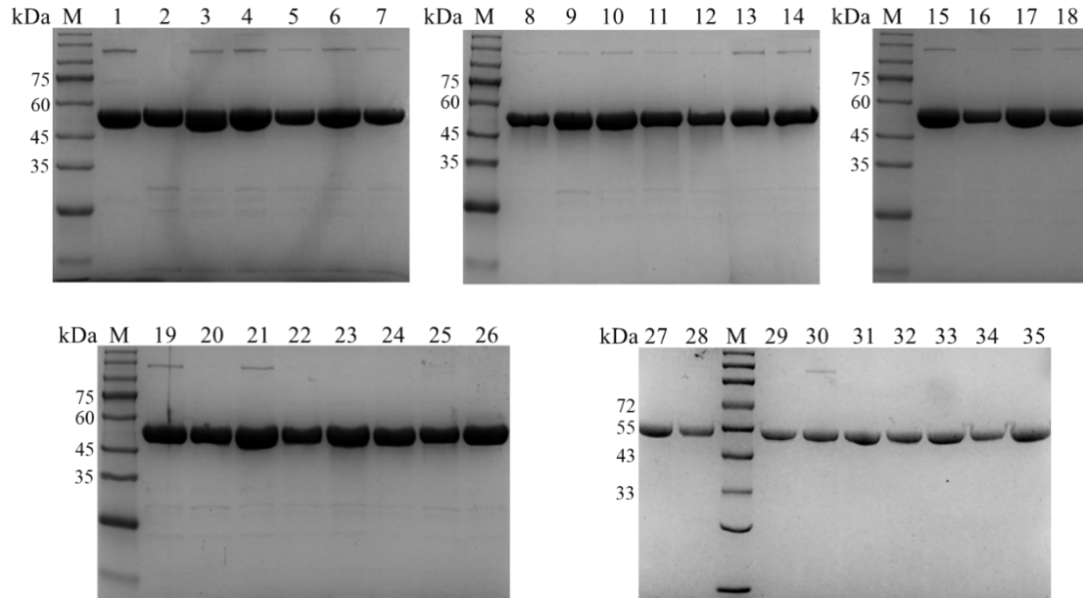


Figure S10. SDS-PAGE analysis of BruN and some of its variants. (A) Lane 1, BruN (expected 53.0 kDa); Lane 2, BruN^{N245V}; Lane 3, BruN^{N441M}; Lane 4, BruN^{N441W}; Lane 5, BruN^{R452V}; Lane 6, BruN^{N441M/R452V}; Lane 7, BruN^{N441W/R452V}; Lane 8, BruN^{F55W}; Lane 9, BruN^{R58V}; Lane 10, BruN^{F243G}; Lane 11, BruN^{N441W/R58V}; Lane 12, BruN^{N441W/F55W}; Lane 13, BruN^{N441M/V440I}; Lane 14, BruN^{N441M/D436P}; Lane 15, BruN^{N441W/F243G}; Lane 16, BruN^{N441W/N245V}; Lane 17, BruN^{N441M/R58V}; Lane 18, BruN^{N441W/V347A}; Lane 19, BruN^{N441W/R452V/V347A}; Lane 20, BruN^{N441W/R452V/D436P}; Lane 21, BruN^{N441W/R452V/F243G}; Lane 22, BruN^{N441W/R452V/V440I}; Lane 23, BruN^{AA/R452V/V347A/CC/F55W/R58V}; Lane 24, BruN^{BB/R452V/V347A/CC/F55W/R58D}; Lane 25, BruN^{AA/R452V/V347A/CC/F55W/R58V/A164L}; Lane 26, BruN^{BB/R452V/V347A/CC/F55W/R58D/I91H}. Lane 27, BruN^{N441F}; Lane 28, BruN^{N441P}; Lane 29, BruN^{N441F/R452V}; Lane 30, BruN^{N441F/A164L}; Lane 31, BruN^{N441F/Q437A}; Lane 32, BruN^{N441F/V440I}; Lane 33, BruN^{N441F/V347L}; Lane 34, BruN^{N441F/Q437P}; Lane 35, BruN^{N441F/Q437A/V347L}; *AA* stands for the multiple-site mutation with T435I/D436P/V440I/N441W/F442G, and *BB* and *CC* for the counterparts with T435I/D436P/Q437A/F439W/V440I/N441M/F442G and F243G/G244P/N245V/K246R/M247V, respectively.

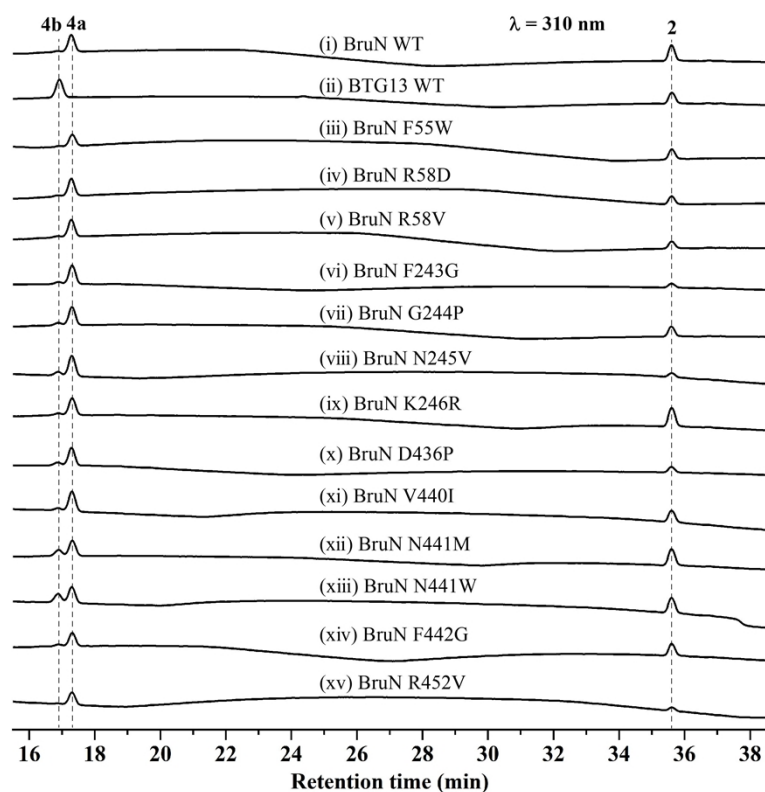


Figure S11. HPLC profiling of chrysophanol (**2**)-derived products under the catalysis of some of single-site BruN variants in the presence of BruM and NADPH.

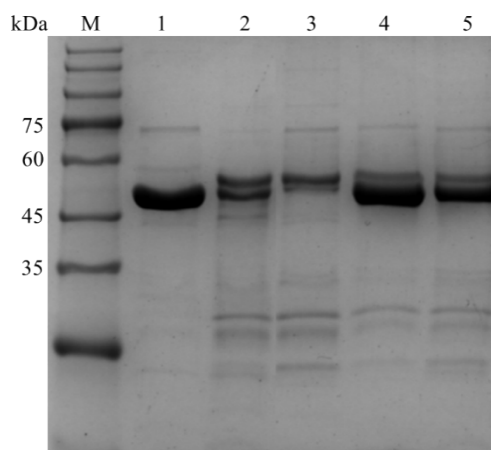


Figure S12. SDS-PAGE analysis of BTG13 and its variants. (A) Lane 1, BTG13 (WAU16873.1, 51.6 kDa); Lane 2, BTG13^{M427N}; Lane 3, BTG13^{M427V}; Lane 4, BTG13^{M427F}; Lane 5, BTG13^{M427P}.

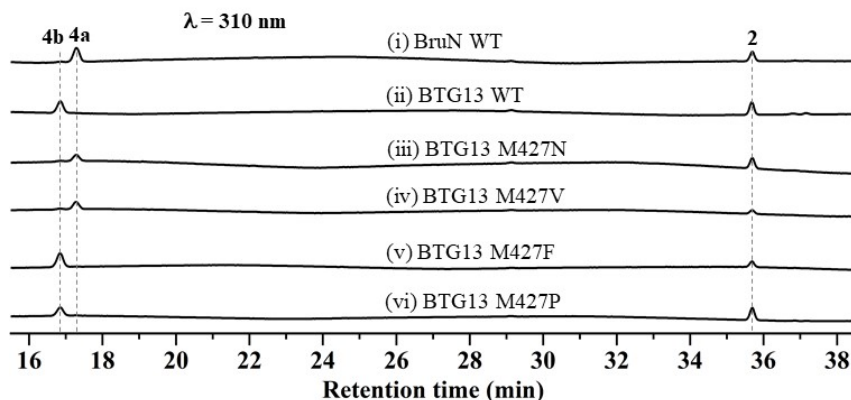


Figure S13. HPLC profiling for monodictyphenone (**4a**) and cephalanone F (**4b**) forming possibly from chrysophanol (**2**) under the catalysis of BTG13 variants in the presence of BruM and NADPH (as cofactor). Each experiment was performed at 30°C for 2 h.

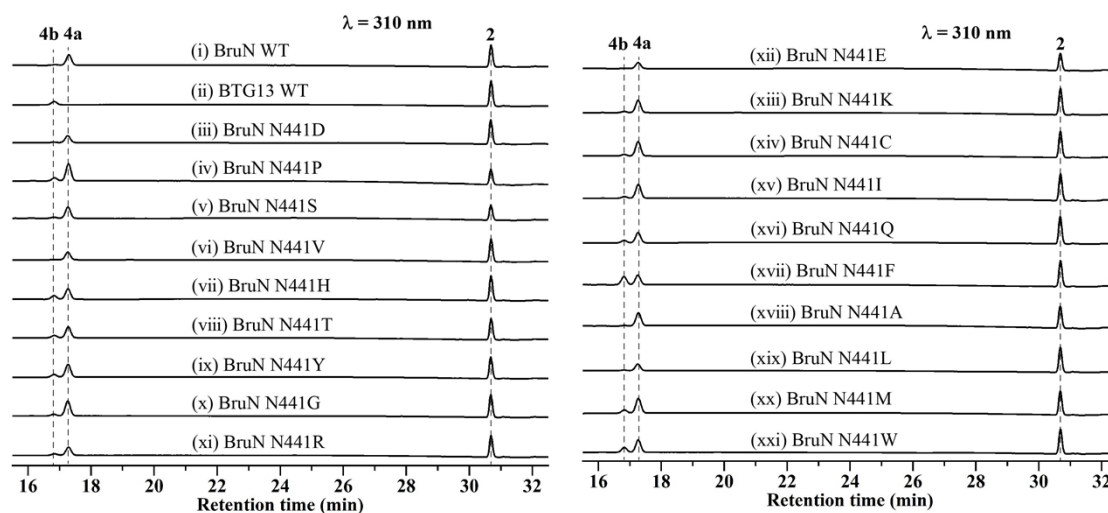


Figure S14. HPLC profiling of chrysophanol (**2**)-derived products under the catalysis of saturation mutants on site N441 in BruN in the presence of BruM and NADPH. The LC-MS analysis was performed using the duration-dependent methanol/water (containing 0.1% formic acid) gradients (0→10 min, 5:95→35:65; 10→18 min, 35:65→56:44; 18→25 min, 56:44→100:0; 25→35 min, pure methanol).

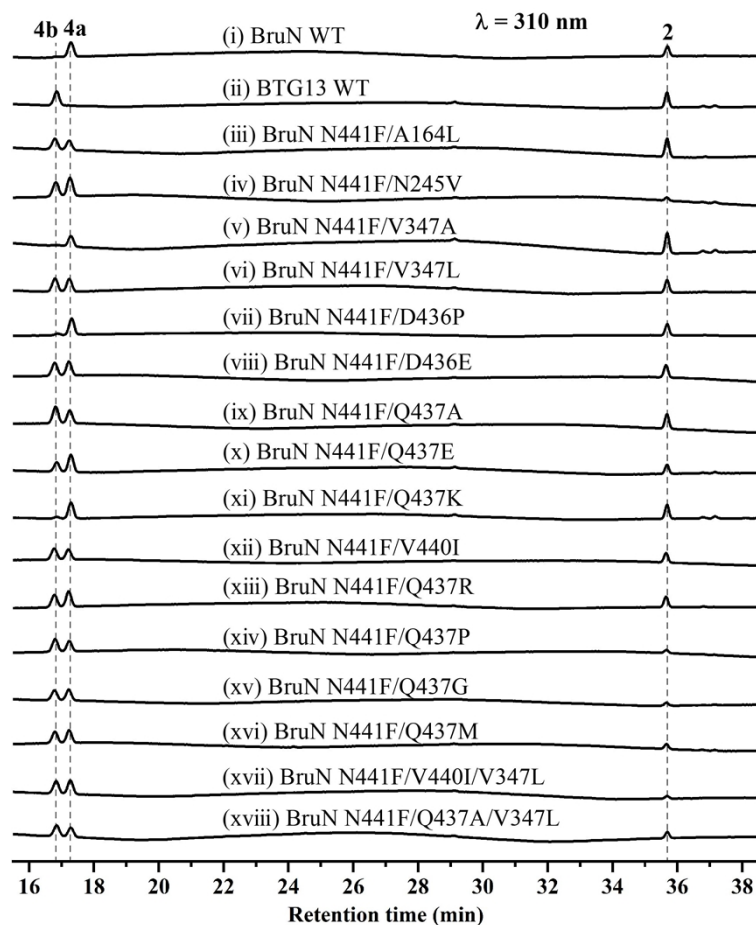


Figure S16. HPLC profiling of chrysophanol (**2**)-derived products under the catalysis of N441-to-phenylalanine muted BruN variants in the presence of BruM and NADPH. Other mutants such as BruN^{N441F/F55W}, BruN^{N441F/R58V}, BruN^{N441F/I91H}, BruN^{N441F/F243G}, BruN^{N441F/G244P}, BruN^{N441F/N245A}, BruN^{N441F/K246R}, BruN^{N441F/M247V}, BruN^{N441F/T435I}, BruN^{N441F/F442G}, BruN^{N441F/D436Q}, BruN^{N441F/Q437N}, BruN^{N441F/Q437W}, BruN^{N441F/Q437F}, BruN^{N441F/Q437L}, BruN^{N441F/Q437Y}, BruN^{N441F/Q437H}, BruN^{N441F/Q437V}, and BruN^{N441F/Q437I} exhibited regioselectivity reversion poorer than that of BruN^{N441F}, that is with the **4a/4b** ratios higher than 54:46.

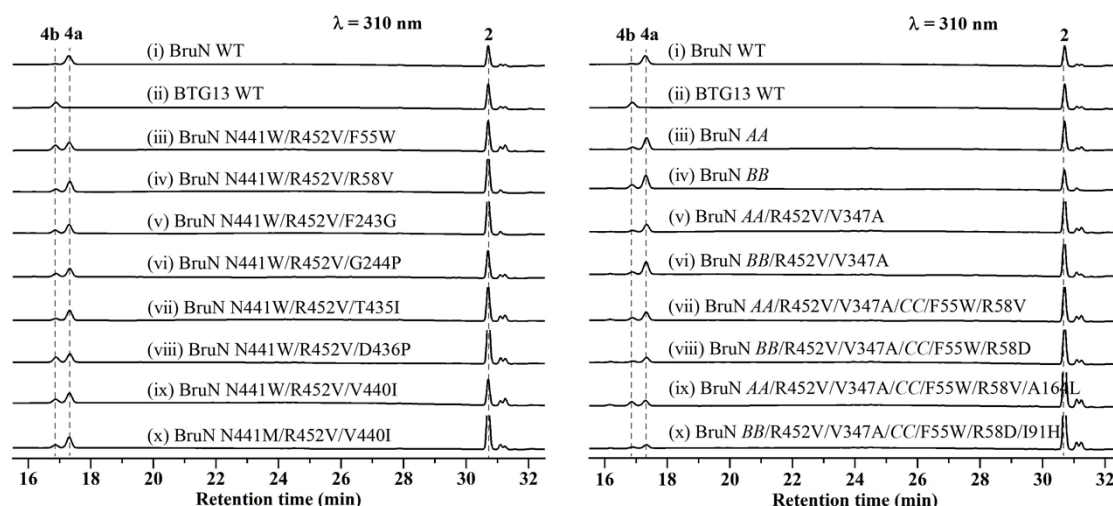


Figure S17. HPLC profiling of chrysophanol (**2**)-derived products under the catalysis of some of multiple-site BruN variants in the presence of BruM and NADPH. *AA* stands for the multiple-site mutation with T435I/D436P/V440I/N441W/F442G, and *BB* and *CC* for the counterparts with T435I/D436P/Q437A/F439W/V440I/N441M/F442G and F243G/G244P/N245V/K246R/M247V, respectively. The LC-MS analysis was performed using the duration-dependent methanol/water (containing 0.1% formic acid) gradients (0→10 min, 5:95→35:65; 10→18 min, 35:65→56:44; 18→25 min, 56:44→100:0; 25→35 min, pure methanol).

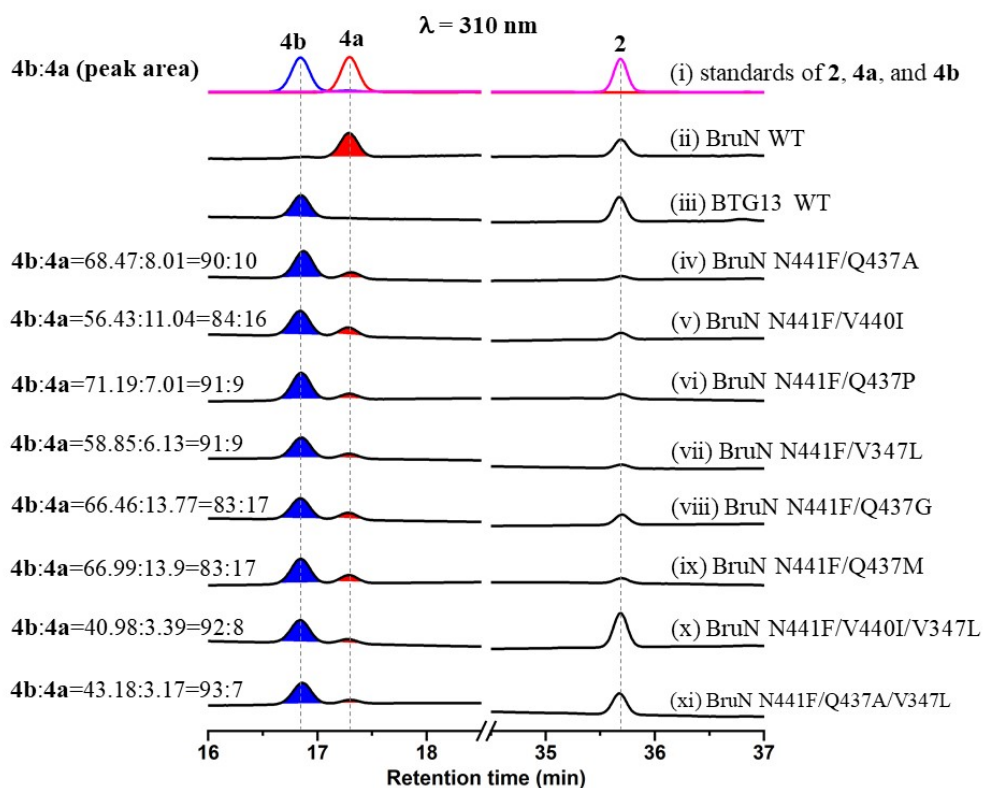


Figure 18. HPLC profiling for monodictyphenone (**4a**) and cephalanone F (**4b**) generating from chrysophanol (**2**) under the catalysis of BruN variants. Peak areas used to calculate **4a/4b** ratios were quantified by the LC-MS analysis.

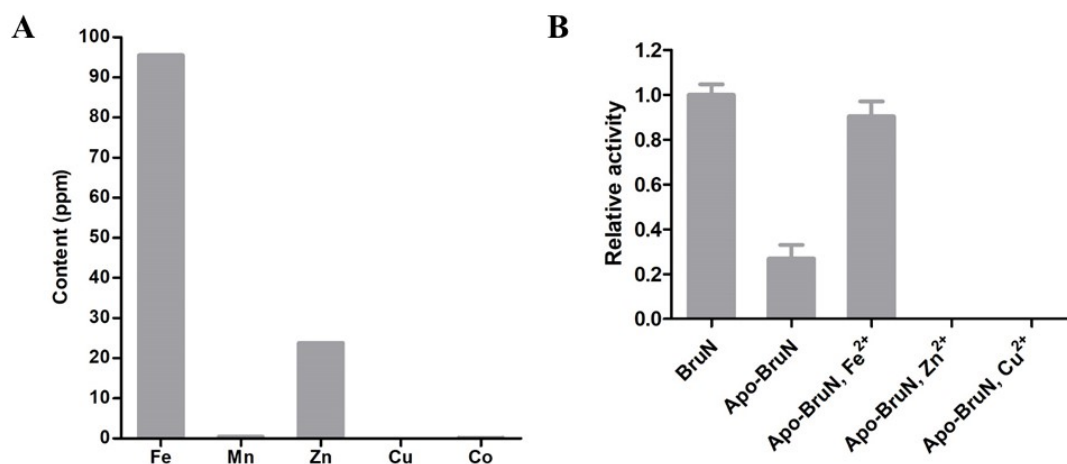


Figure S19. Identification of the BruN-bound iron ion. (A) ICP-MS analysis for the BruN binding with metal ion candidates. (B) Catalytic competence fluctuation of BruN with its Fe ion replacement by other divalent metals using aloe emodin (**5**) as substrate in the presence of BruM and NADPH.

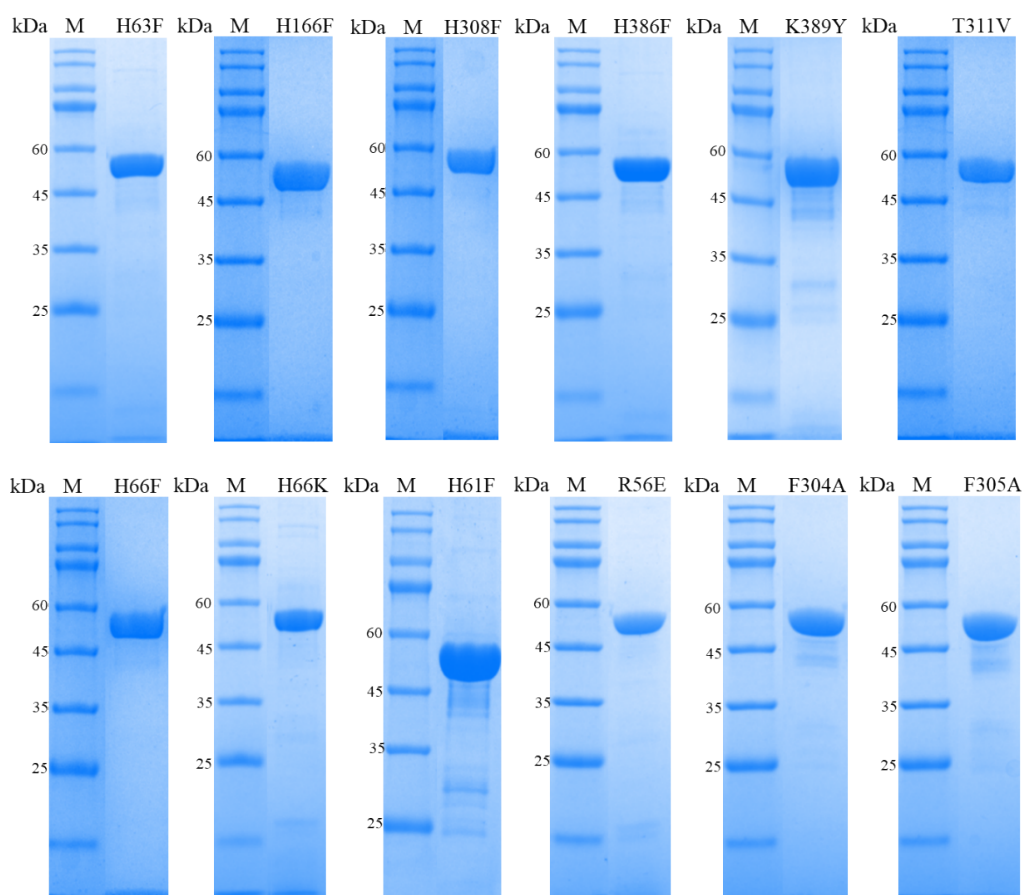


Figure S20. SDS-PAGE analysis of purified BruN variants (53.0 kDa) resulting from mutating the conserved and functionally significant sites as co-indicated by the multiple sequence alignment (see Figure S8) and the docking result of BruN with chrysophanol hydroquinone (**3**) (see Figure 3B).

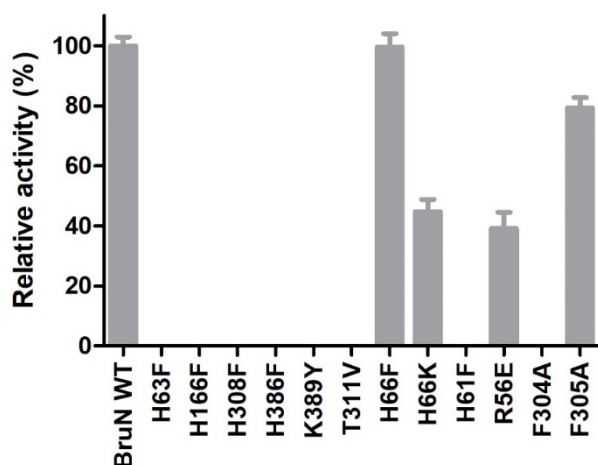


Figure S21. Activity comparison for BruN and its mutants in catalyzing the chrysophanol (**2**) cleavage in the presence of BruM and NADPH.

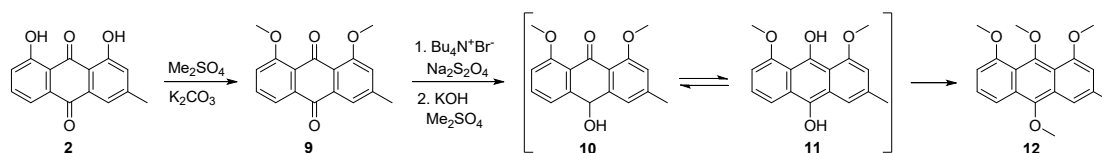


Figure S22. Compound **12** was synthesized from chrysophanol (**2**) to confirm the keto-enol tautomerism that might be involved in the enzymatic fission process.

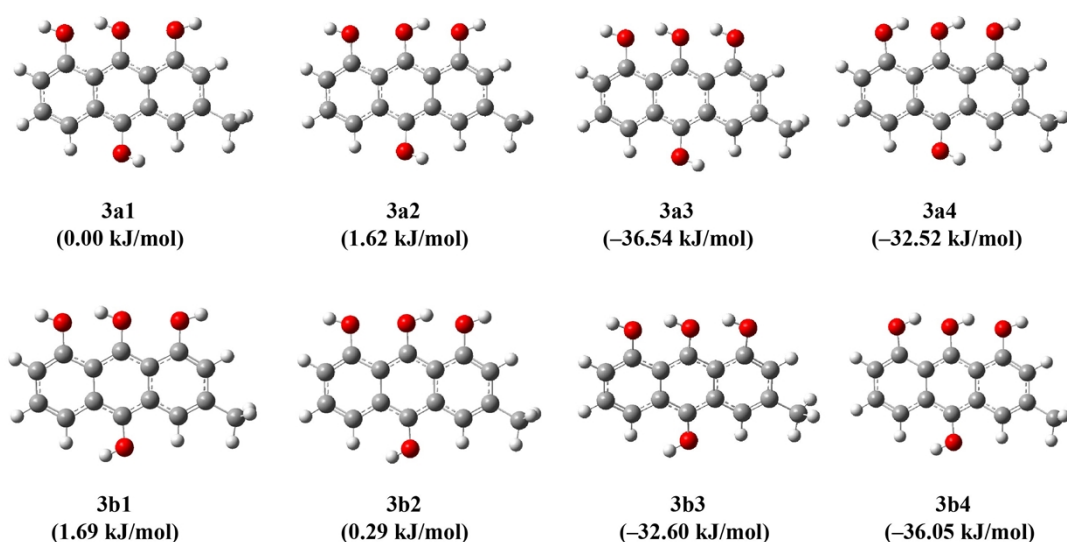


Figure S23. Conformations of **3a** and **3b** with their relative energies obtained at B3LYP level.

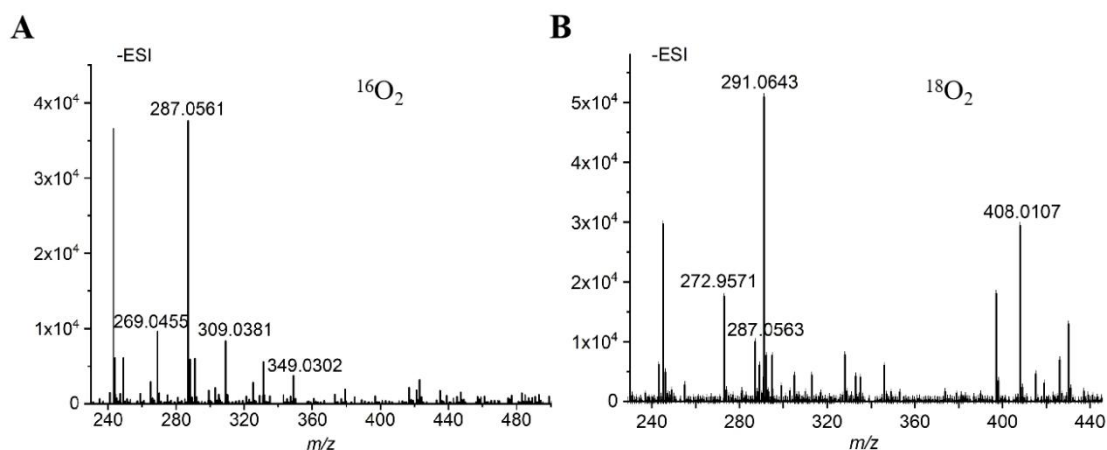


Figure S24. HR-ESI-MS spectra of monodictyphenone (**4a**) produced in atmospheric $^{16}\text{O}_2$ (A) and $^{18}\text{O}_2$ (B). In simultaneous exposure to BruMN and NADPH, **2** was separately oxidized by atmospheric $^{16}\text{O}_2$ and $^{18}\text{O}_2$ to generate normal (unlabeled) and isotopically labeled products (**4a**) with the quasimolecular ($[\text{M} - \text{H}]^-$) ions displayed at m/z 287.0561 (A) and 291.0643 (B), respectively.

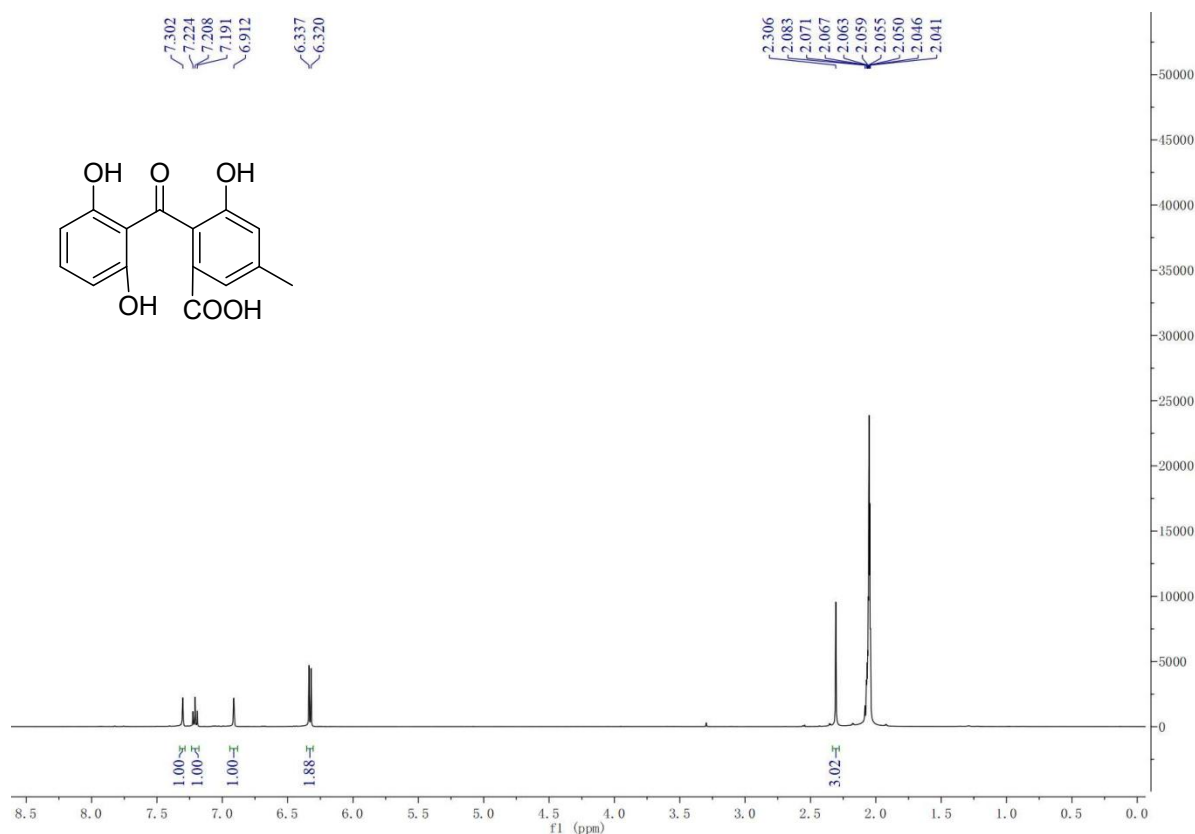


Figure S25. ^1H NMR spectrum of monodictyphenone (**4a**).

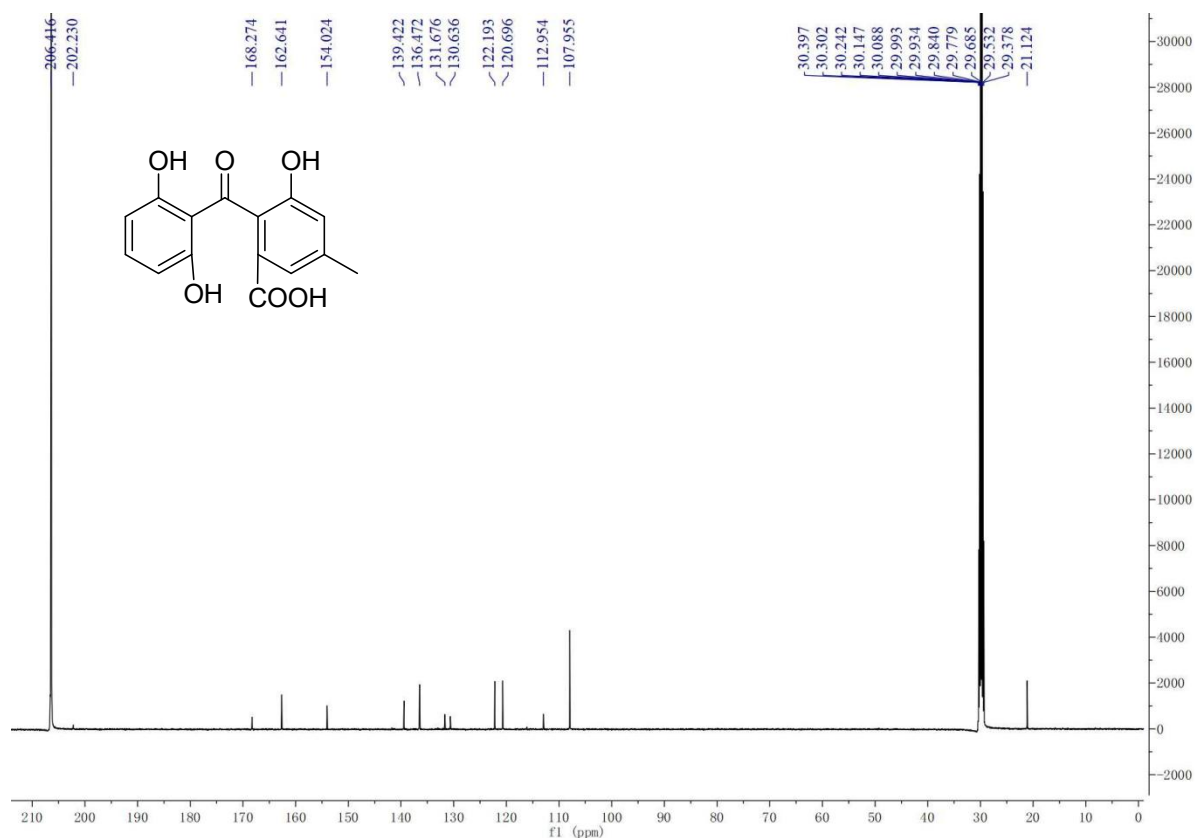


Figure S26. ^{13}C NMR spectrum of monodictyphenone (**4a**).

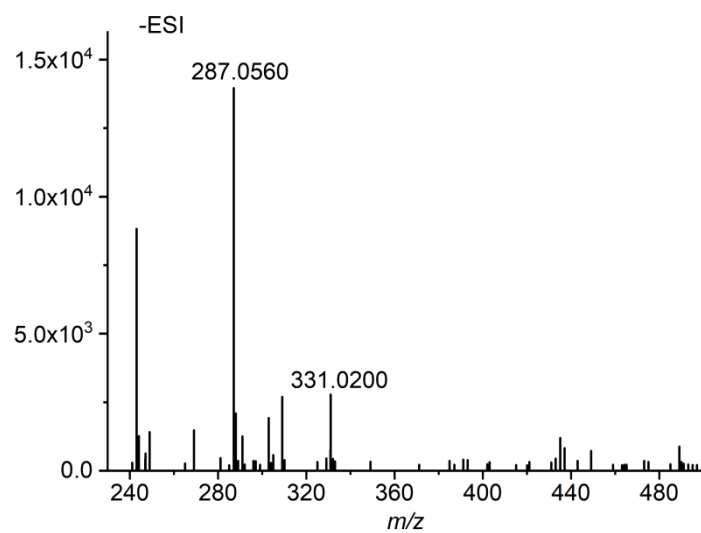


Figure S27. HR-ESI-MS spectrum of cephalanone F (**4b**).

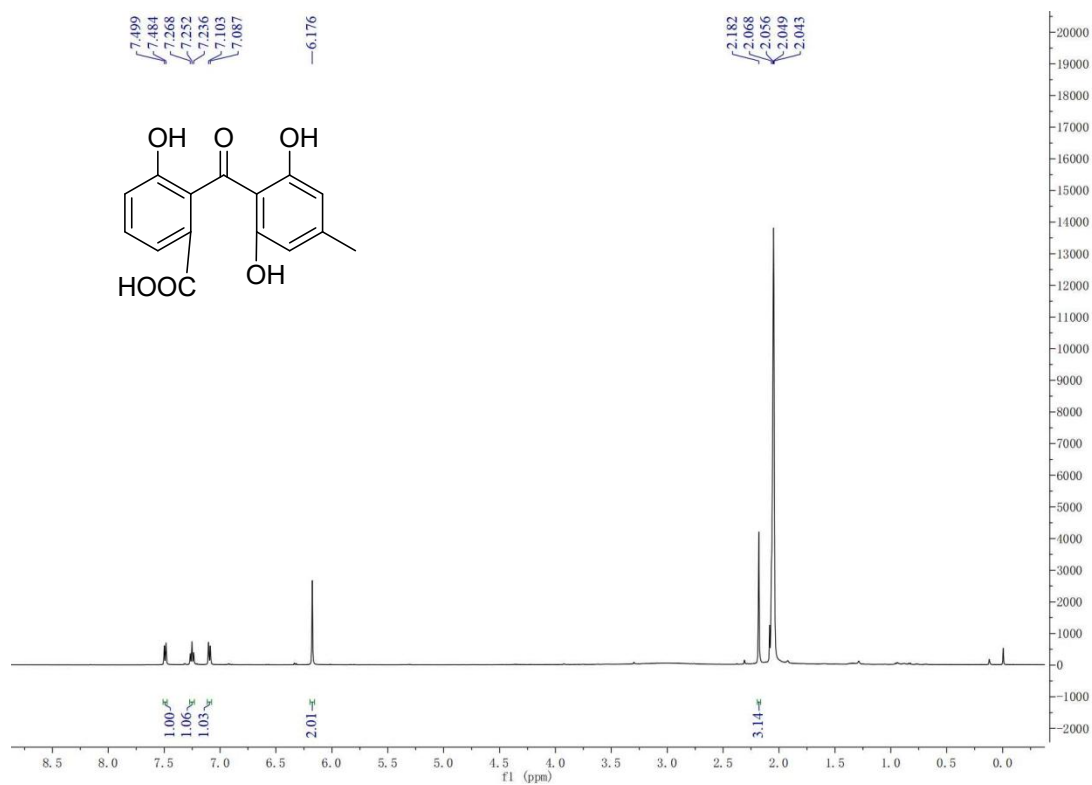


Figure S28. ¹H NMR spectrum of cephalanone F (**4b**).

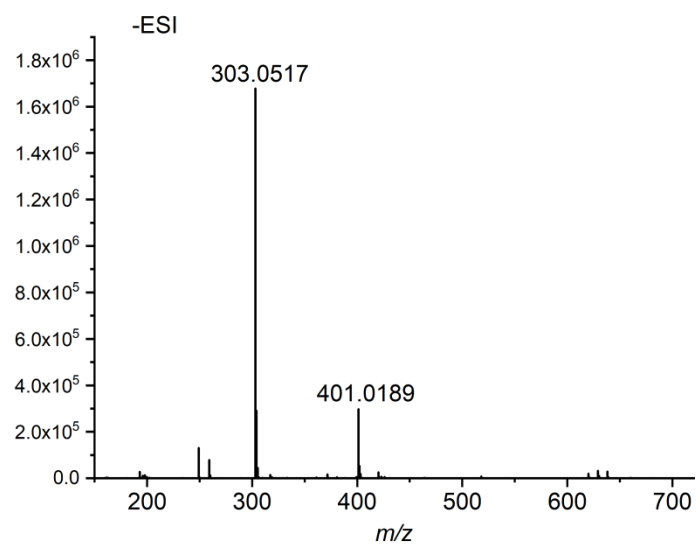


Figure S29. HR-ESI-MS spectrum of 11-hydroxy monodictyphenone (**5a**).

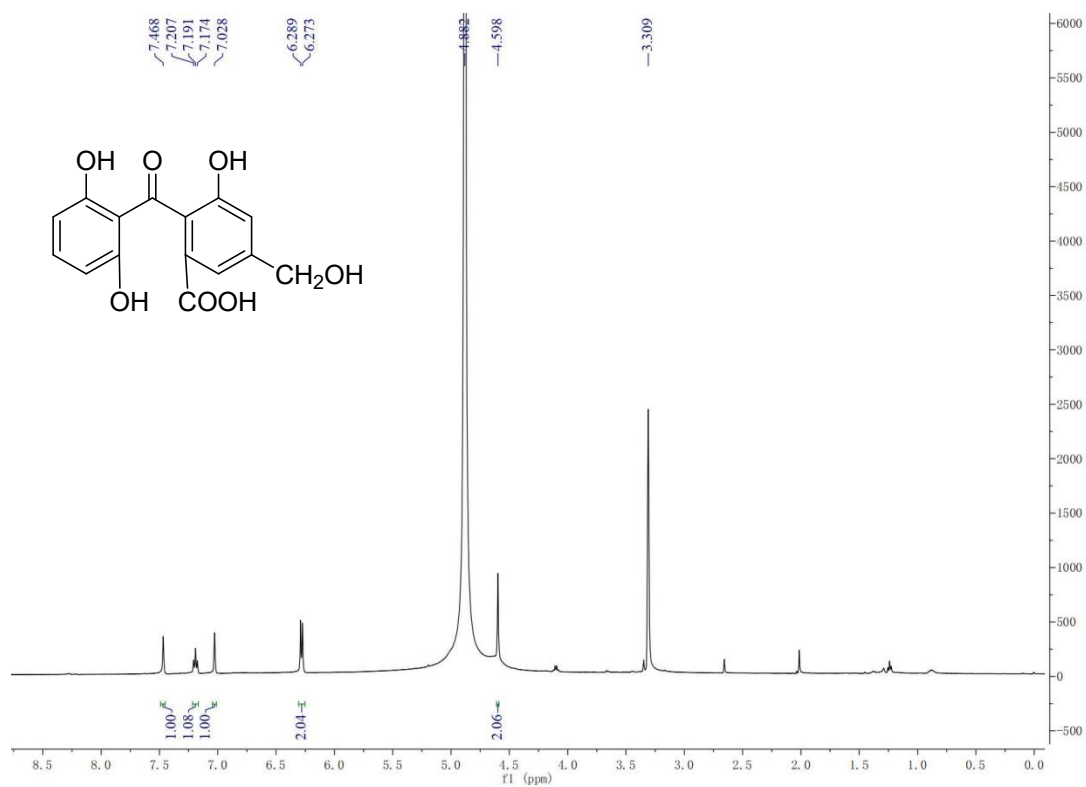


Figure S30. ^1H NMR spectrum of 11-hydroxy monodictyphenone (**5a**) in CD_3OD .

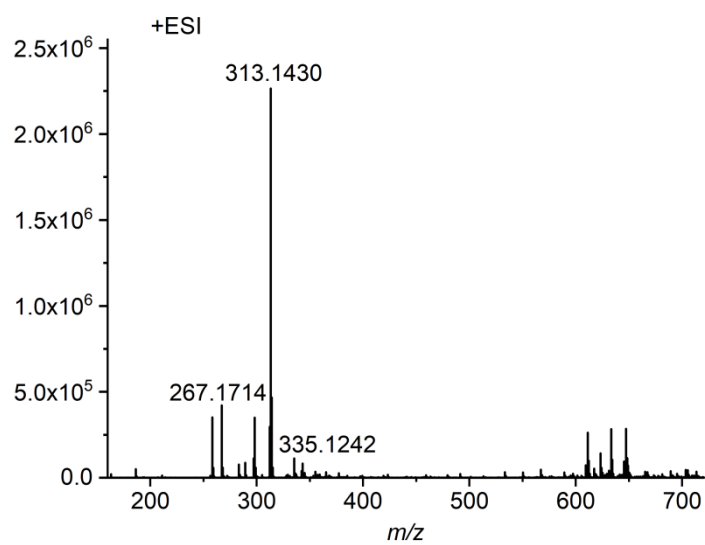


Figure S31. HR-ESI-MS spectrum of **12**.



Figure S32. ^1H NMR spectrum of **12** in CDCl_3 .



Figure S33. ^{13}C NMR spectrum of **12** in CDCl_3 .

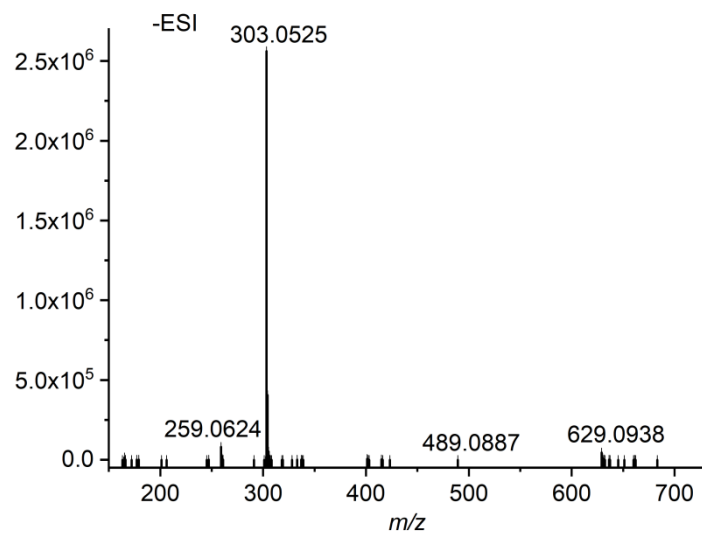


Figure S34. HR-ESI-MS spectrum of emodinic acid.

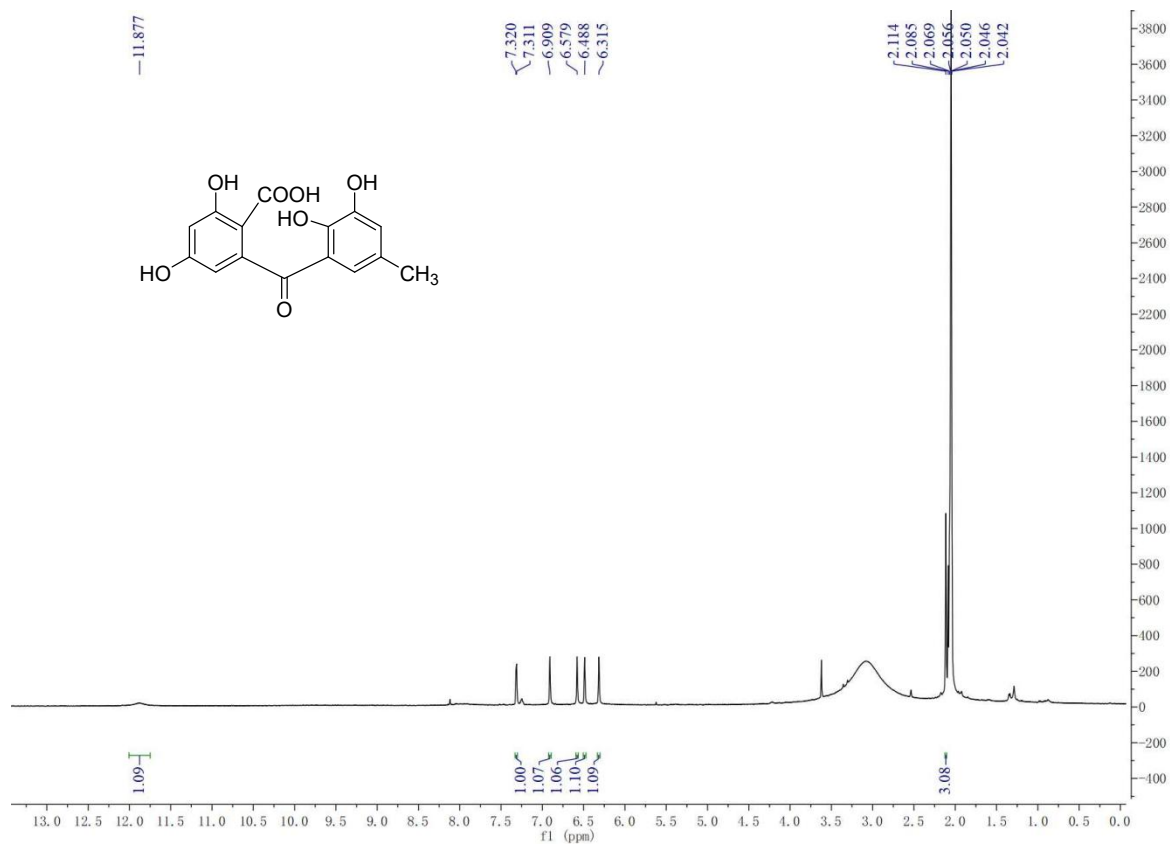


Figure S35. ^1H NMR spectrum of emodinic acid.

References

- 1 X. J. Lv, F. Ding, Y. J. Wei and R. X. Tan, *Chin. J. Chem.*, 2021, **39**, 1580–1586.
- 2 K. Blin, S. Shaw, K. Steinke, R. Villebro, N. Ziemert, S. Y. Lee, M. H. Medema and T. Weber, *Nucleic Acids Res.*, 2019, **47**, W81–W87.
- 3 F. N. Gravelat, D. S. Askew and D. C. Sheppard, *Methods Mol. Biol.*, 2012, **845**, 119–130.
- 4 X. D. Hou, H. B. Xu, Z. W. Deng, Y. J. Yan, Z. B. Yuan, X. Z. Liu, Z. P. Su, S. Yang, Y. Zhang and Y. J. Rao, *Angew Chem. Int. Edit.*, 2022, **61**, e202208772.
- 5 Y. S. Wang, B. Zhang, J. P. Zhu, C. L. Yang, Y. Guo, C. L. Liu, F. Liu, H. Q. Huang, S. W. Zhao, Y. Liang, R. H. Jiao, R. X. Tan and H. M. Ge, *J. Am. Chem. Soc.*, 2018, **140**, 10909–10914.
- 6 S. W. Yuan, S. H. Chen, H. Guo, L. T. Chen, H. J. Shen, L. Liu and Z. Z. Gao, *Org. Lett.*, 2022, **24**, 3069–3074.
- 7 X. X. Wei, X. X. Chen, L. Chen, D. X. Yan, W. G. Wang and Y. Matsuda, *J. Nat. Prod.*, 2021, **84**, 1544–1549.
- 8 Y. M. Chiang, E. Szewczyk, A. D. Davidson, R. Entwistle, N. P. Keller, C. C. C. Wang and B. R. Oakley, *Appl. Environ. Microbiol.*, 2010, **76**, 2067–2074.
- 9 A. J. Szwalbe, K. Williams, Z. S. Song, K. de Mattos-Shiple, J. L. Vincent, A. M. Bailey, C. L. Willis, R. J. Cox and T. J. Simpson, *Chem. Sci.*, 2019, **10**, 233–238.
- 10 L. Neubauer, J. Dopstadt, H. U. Humpf and P. Tudzynski, *Fung. Biol. Biotechnol.*, 2016, **3**, 2.
- 11 C. Greco, K. de Mattos-Shiple, A. M. Bailey, N. P. Mulholland, J. L. Vincent, C. L. Willis, R. J. Cox and T. J. Simpson, *Chem. Sci.*, 2019, **10**, 2930–2939.
- 12 F. F. Qi, W. Zhang, Y. Y. Xue, C. Geng, X. N. Huang, J. Sun and X. F. Lu, *J. Am. Chem. Soc.*, 2021, **143**, 16326–16331.
- 13 K. Throckmorton, F. Y. Lim, D. P. Kontoyiannis, W. F. Zheng and N. P. Keller, *Environ. Microbiol.*, 2016, **18**, 246–259.
- 14 X. X. Xu, L. Liu, F. Zhang, W. Z. Wang, J. Y. Li, L. D. Guo, Y. S. Che and G. Liu, *ChemBioChem.*, 2014, **15**, 284–292.
- 15 Y. Matsuda, C. H. Gotfredsen and T. O. Larsen, *Org. Lett.*, 2018, **20**, 7197–7200.
- 16 S. Kumar, G. Stecher, M. Li, C. Knyaz and K. Tamura, *Mol. Biol. Evol.*, 2018, **35**, 1547–1549.
- 17 J. Abramson, J. Adler, J. Dunger, R. Evans, T. Green, A. Pritzel, O. Ronneberger, L. Willmore, A. J. Ballard, J. Bambrick, S. W. Bodenstein, D. A. Evans, C. C. Hung, M. O’Neill, D. Reiman, K. Tunyasuvunakool, Z. Wu, A. Zemgulyte, E. Arvaniti, C. Beattie, O. Bertolli, A. Bridgland, A. Cherepanov, M. Congreve, A. I. Cowen-Rivers, A. Cowie, M. Figurnov, F. B. Fuchs, H. Gladman, R. Jain, Y. A. Khan, C. M. R. Low, K. Perlin, A. Potapenko, P. Savy, S. Singh, A. Stecula, A. Thillaisundaram, C. Tong, S. Yakneen, E. D. Zhong, M. Zielinski, A. Zidek, V. Bapst, P. Kohli, M. Jaderberg, D. Hassabis and J. M. Jumper, *Nature*, 2024, **630**, 493–500.
- 18 A. Krick, S. Kehraus, C. Gerhäuser, K. Klimo, M. Nieger, A. Maier, H. H. Fiebig, I. Atodiresei, G. Raabe, J. Fleischhauer and G. M. König, *J. Nat. Prod.*, 2007, **70**, 353–360.
- 19 T. Asai, S. Otsuki, H. Sakurai, K. Yamashita, T. Ozeki and Y. Oshima, *Org. Lett.*, 2013, **15**, 2058–2061.
- 20 C. Terreaux, Q. Wang, J. R. Ioset, K. Ndjoko, W. Grimminger and K. Hostettmann, *Planta Med.*, 2002, **68**, 349–354.
- 21 H. Miyabe, M. Torieda, K. Inoue, K. Tajiri, T. Kiguchi and T. Naito, *J. Org. Chem.*, 1998, **63**,

4397–4407.

- 22 Y. B. Han, W. Bai, C. X. Ding, J. Liang, S. H. Wu and R. X. Tan, *J. Am. Chem. Soc.*, 2021, **143**, 14218–14226.